TÉCNICO LISBOA

Fast aerodynamic design of a one-stage axial gas turbine in order to produce a 3D geometry ready for optimization

Artur João Carvalho Batista Soares de Figueiredo

Thesis to obtain the Master of Science Degree in

Aerospace Engineering

Supervisor

Professor Afzal Suleman

Examination Committee

Chairperson: Professor Fernando José Parracho Lau

Supervisor: Professor Afzal Suleman

Member of the Committee: Professor João Manuel Melo de Sousa

October 2014

To my Mother, for all the help given at all times

The Wright Brothers created the single greatest cultural force since the invention of writing. The airplane became the first World Wide Web, bringing people, languages, ideas, and values together.

Bill Gates

Acknowledgements

The fulfilment of this thesis would have been impossible without the help of many people. Therefore, I must express my thanks:

To my supervisor at Von Karman Institute for Fluid Dynamics, Professor Tony Arts, for his patience, wisdom and guidance throughout my six months at VKI;

To my supervisor at Instituto Superior Técnico of Lisbon, Professor Afzal Suleman, for taking care of the necessary arrangements so that I could conduct my Master's thesis at VKI (including a recommendation letter) and for presenting my thesis at IST Lisbon;

To Zuyher Alsalihi, with whom I compared the results of the *C* program hereby developed, and hence helped me find mistakes and make improvements in the code;

To Lasse Müller, for kindly allowing me to use his improved figures for the Craig & Cox correlation;

To Professor Filipe Cunha, for sharing his experience at VKI and for one of the recommendation letters that allowed me to apply for this institute;

To Professor Fernando Lau, for (more than once) helping me with the documents always necessary for conducting a period of study abroad;

To Instituto Superior Técnico, for preparing me as an engineering student as I wouldn't be prepared anywhere else;

To Von Karman Institute for Fluid Dynamics, for all the shared knowledge and the inviting and friendly work environment;

To Technische Universiteit Delft, for the engineering insights and for my first introduction to Turbomachinery and engines in general;

To my friends, who have, in some way, assisted me in conducting my Master's Thesis at VKI, Alberto Serrano, Bruno Dias, Charline Fouchier, David Cuadrado, João Aguiar, José Veiga, Marília Avelar, Pedro Santos, Rui Jaulino, Tiago Barros and Valeria Andreoli;

To my Mother, Cândida Perpétua Carvalho, for all the help given at all times.

Brussels, October 2014

Abstract

The turbine plays a vital role in major industries worldwide, namely in electricity generation and the aerospace industry. The preliminary design phase of a turbine (one of most important phases of the overall design, since it sets the tone for all subsequent design stages and results) is nowadays often carried out by hand. However, in any industry, reducing costs and increasing efficiency are everyday goals. The need for an automatic, fast and reliable way to perform a preliminary design of an axial turbine in order to produce a 3D geometry ready for optimization brings us to the purpose of this thesis.

The necessary tools for such a preliminary design are nowadays accepted knowledge for any turbine designer. The purpose of this work is to use this knowledge for the creation of a methodology, coded into a *C* program, capable of delivering a feasible and realistic turbine preliminary design ready for optimization, starting only with data from the engine this turbine belongs to.

Typical thermodynamic analysis of an engine (turboshaft), followed by the application of mean line analysis and radial equilibrium theory (ISRE and NISRE) and subsequent airfoil selection compose the main tools in this design. Loss calculation is included with Soderberg's correlation in the 1D design (MLA), and with Craig & Cox's method in the 2D design (RET).

The objective of this thesis was therefore attained, with the development of a methodology able to deliver a full 2D design of a turbine and consequently a 3D geometry.

Keywords: turbine design, preliminary, MLA, RET, airfoil.

Resumo

A turbina desempenha um papel crucial nas maiores indústrias mundiais, nomeadamente na produção de electricidade e na indústria aeroespacial. A fase preliminar do projecto de uma turbina (uma das fases mais importantes, já que influencia todas as subsequentes fases do projecto e respectivos resultados) continua, frequentemente, a ser realizada à mão. No entanto, em qualquer indústria, reduzir os custos e aumentar a eficiência são objectivos diários. O objectivo desta tese prende-se com a necessidade de um processo automático, rápido e fiável de obter o projecto preliminar de uma turbina axial com vista a produzir uma geometria 3D pronta para optimização.

As ferramentas necessárias para o projecto preliminar são hoje em dia conhecimento aceite para a comunidade científica. O objectivo deste trabalho é usar este conhecimento para a criação de uma metodologia, e consequente programa em *C*, capaz de retornar um projecto preliminar de uma turbina exequível e realista pronto para ser optimizado, usando apenas dados do motor no qual a turbina está inserida.

Uma simples análise termodinâmica do motor (*turboshaft*), seguida de uma *mean line analysis* e *radial equilibrium theory* (*ISRE* and *NISRE*) e de uma escolha de perfis, constituem as principais ferramentas para efectuar este projecto. O cálculo das perdas está também incluído, usando a correlação de Soderberg no design 1D(MLA) e depois o método de *Craig & Cox* no design 2D(RET).

O objectivo deste tese foi cumprido, com o desenvolvimento de um programa capaz de retornar um projecto preliminar 2D de uma turbina e consequente geometria 3D.

Palavras-chave: projecto de turbina, preliminar, MLA, RET, perfil.

Contents

List of Figures

List of Tables

Nomenclature

Acronyms

Symbol	*Description*
1D	one-dimensional
2D	two-dimensional
3D	three-dimensional
ECA	Engine Cycle Analysis
ISRE	Isentropic Simple Radial Equilibrium
MLA	Mean Line Analysis
NISRE	Non-Isentropic Simple Radial Equilibrium
RET	Radial Equilibrium Theory

Latin Symbols

Symbol	*Unit*	*Description*
A	m^2	area
A_k	m^2	total effective area of clearance
A_t	m^2	total blade throat area
a	m/s	speed of sound
b	m	blade backbone length
C_{l_0}	-	camber, expressed as design lift coefficient of isolated airfoil
CR	-	contraction ratio
c	m	chord
c_x	m	axial chord
c_p	$J/(kg.K)$	specific heat at constant pressure
Dh	m	hydraulic diameter
d	m	diameter
e	m	back surface radius
F_k	-	efficiency debit factor
F_L	-	lift parameter
g	m	pitch
$(g/c)_0$	-	optimum pitch to chord ratio at zero trailing edge thickness

$g_{M=0.8}$	m	optimum pitch at non-zero trailing edge thickness
g_M	m	optimum pitch after Mach number correction
h	J/kg	specific enthalpy
h	m	blade height
i	rad	incidence angle
LER	m	leading edge radius
LHV	J/kg	Lower heating value
M	-	Mach number
ml	m	mean line (camber line) length
$\dot{m}$	kg/s	mass flow
N_b	-	number of blades
N_{pr}	-	profile loss ratio against Reynolds number effect
N_{pt}	-	profile loss ratio against trailing edge thickness
N_{pi}	-	profile loss ratio against incidence angle
$(N_s)_{h/b}$	-	secondary loss ratio against aspect ratio factor
$(N_s)_r$	-	secondary loss ratio against Reynolds number effect
K	-	hub to tip secondary losses ratio
o	m	throat size
P	W	power
p	m	level of penetration
p	Pa	pressure
Q	J	heat
R	$J/(kg.K)$	specific gas constant
Re	-	Reynolds number
R_h	-	enthalpy (degree of) reaction
R_p	-	pressure (degree of) reaction
r	m	radius
s	$J/(kg.K)$	specific entropy
T	K	temperature
TER	m	trailing edge radius
t_e	m	trailing edge thickness
t/c	-	blade thickness over chord ratio
U	m/s	rotation velocity
V	m/s	absolute velocity
W	m/s	relative velocity
X	%	total loss factor
X_p	%	profile loss factor
X_s	%	secondary loss factor
x_{pb}	%	basic profile loss parameter

$(x_s)_b$	%	basic secondary loss parameter
$(\Delta\alpha)_c$	°	turning angle of the camber line
$(\Delta\alpha)_{deviation}$	°	angle between leaving flow direction and trailing-edge meanline direction
$(\Delta\alpha)_{induced}$	°	change in direction of the stagnation streamline at the leading edge
$\Delta\eta_k$	-	reduction of blading efficiency due to clearance losses
ΔL	m	clearance length
$(\Delta x_p)_t$	-	profile loss increment due to trailing edge thickness
$(\Delta x_p)_{s/e}$	-	profile loss increment due to blade back radius
$(\Delta x_p)_m$	-	profile loss increment due to Mach number
$\eta_{\substack{zero\\clr.}}$	-	blading efficiency for zero tip clearance

Greek Symbols

Symbol	*Unit*	*Description*
α	rad	absolute flow angle
β	rad	relative flow angle
γ	rad	stagger angle
Δ	-	variation
$\Delta\alpha$	rad	turning angle
ϵ	rad	wall angle
ζ	-	loss in kinetic energy referred to the isentropic velocity
η	-	efficiency
κ	-	heat capacity ratio
μ	Ns/m^2	dynamic viscosity
ξ	-	loss in kinetic energy referred to the real velocity
$\xi^{'}$	-	Soderberg's nominal loss coefficient
$\xi^{''}$	-	Soderberg's aspect ratio correction
$\xi^{'''}$	-	Soderberg's Reynolds number correction
Π	-	pressure ratio
ρ	kg/m^3	density
τ	rad	angle between an airfoil coordinate tangent and the horizontal axis x_a
ϕ	-	flow coefficient
ψ	-	load coefficient
Ω	rad/s	angular velocity
ω	-	total pressure loss coefficient

Subscripts

Symbol	*Description*
0	total conditions
1,2,3,...	control sections
a	airfoil coordinates
air	air conditions
av	available
b	ordinate point
c	camber
c	compressor
CC	Craig & Cox
cc	combustion chamber
cr	critical
f	fuel
gas	gas conditions
gg	gas generator
p	profile
pt	power turbine
R	rotor
r	radial direction
S	stator
s	isentropic
s	secondary
sl	slope
t	thickness
TS	total to static
TT	total to total
w	wall
x	axial direction
θ	meridional direction

Superscripts

Symbol	*Description*
h	hub
h0	point on the hub side where the secondary losses exist no more
l	lower
m	mean
n	new
r	relative

t	tip
t0	point on the tip side where the secondary losses exist no more
u	upper
’	value referred to vane
”	value referred to blade

Engine Numbering

Symbol	*Description*
1	compressor inlet
2	compressor outlet / combustion chamber inlet
3	combustion chamber outlet / gas generator inlet
4	gas generator outlet / power turbine inlet
5	power turbine outlet

Turbine Numbering

Symbol	*Description*
1	stator inlet
2	stator outlet / rotor inlet
3	rotor outlet

Chapter 1

Introduction

From the first recorded steam turbine, the *aeolipile* in the 1^{st} century AD, no more than a small curiosity and without any practical purpose, credited to Heron of Alexandrian [1], to the invention of the modern steam turbine, credited to Sir Charles Algernon Parsons [2], about 18 centuries elapsed. Then, within Sir Charles Parsons' lifetime (1854-1931), the use and development of this steam turbine blossomed. There were plenty of reasons for this fact, namely the fact that Sir Charles Parsons was born in the so called Workshop of the World, as Great-Britain was known at the time, only three years after the Great Exhibition of the Works of Industry of all Nations, which took place in Chrystal Palace, London, 1851. Moreover, he was a son of the famous astronomer, William Parsons, Earl of Rosse, and belonged to a family of well-known engineers and scientists. Parsons' steam turbine played a crucial role in the late Industrial Revolution and Victorian Period. Besides this, he dedicated himself to Marine Steam Turbines and had the *Turbinia* built, a high speed turbine powered yacht, showed off on occasion of Queen Victoria's Diamond Jubilee.

After Great-Britain, all major world power stations adopted this new design, which was improved tremendously over the years and had the ability of being scaled up in a rather easy fashion. Today, reaction turbines are the basis for some of the most powerful and expensive industries in the world, such as electricity generation and the aerospace industry. As in any other industry, reducing costs and increasing efficiency are everyday goals. The turbine, being such an important element, has been the object of intensive study and improvement. Even now, however, a turbine design, and especially, a preliminary design, is greatly influenced by the designer and the choices he/she makes in this design stage. Hence, still nowadays, preliminary designs are usually hand-made. This steals time in a direct way, since this design phase could have been conducted with computer calculation power, and in an indirect way, since improving this preliminary design would be much easier with an already partly optimized and limited design space. This need for an automatic, fast and reliable way to perform a preliminary design of an axial turbine brings us to purpose of this thesis.

1.1 Context and Motivations

This document and the associated C program were developed during a 6 month internship at VKI, von Karman Institute for Fluid Dynamics, within the Turbomachinery and Propulsion Department. This internship was essential for receiving "first-hand" designing experience which was not available through the common resources, including essential knowledge for the modelling and prediction of certain aspects of the turbine, as typically happens in a preliminary design phase. In fact, since at the same time another program was being created at VKI with the same purpose of turbine preliminary design (although with a different procedure), it was possible to compare results in order to assure the veracity of the output delivered by the C program hereby developed.

Turbine design and turbines in general are of particular importance to the Aerospace field, with requirements for efficiency and less fuel consumption driving a new era of improvement in design, maintenance and development of this element. It is estimated that worldwide, every year, about a thousand gas turbines are sold. This number is bound to increase, with the Aerospace sector experiencing an increase in demand, making the number of airliners in service increase every year.

Hence, for all these reasons, the understanding of design strategies concerning gas turbines is of utmost importance for a rapid, constantly changing and demanding World, where providing a customer with fast and positive answers is a requirement for success, as well as a task of science.

1.2 Design Task and Objectives

The objective of this thesis is to develop a methodology that allows a user to obtain a one-stage gas turbine 3D geometry ready for optimization, starting from global data. The program developed should be as user friendly as possible, enabling any user to obtain an efficient turbine design for any data, such as compressor pressure ratio, turbine total inlet temperature, among others, given as input.

Therefore, the main objectives of this thesis concern the understanding of the engine cycle analysis and mean line analysis (1D design), including the influence of each variable on feasibility and output power; the understanding of radial equilibrium theory (2D design) and its application in order to obtain a good radial design of the turbine in study; and the understanding of the process of airfoil choosing. In fact, contained in the items previously presented, is also the study of historical trends and good practices of turbine design, knowledge passed to the C program developed during this thesis, along with different models for loss calculation in a turbine.

Accomplishing these objectives should allow for the development of a program able to compute a feasible turbine design starting from simple global data.

1.3 State of the Art and Literature Review

Gas turbines have had a long and replenished history, starting, as referred before, around the 1^{st} century AD. Several people have made a contribution to help make gas turbines what they are today. One can say that it was indeed team work that produced such an important element for modern civilization. The

three laws of motion, published by Sir Isaac Newton, are the foundation for modern propulsion theory and therefore, the most important building block in the development of the gas turbine. Several designs, with new innovations and improvements were patented throughout the years, with the first being credited to John Barber [3], even though his turbine was designed to power a horseless carriage. About 100 years afterwards, another Englishman, Sir Charles Parsons, patented a new turbine. His main contribution was the objective of his turbine. The idea was to propel a ship using the steam turbine power, or to generate electricity through it. That was a major breakthrough for the use of turbines in the transportation industry and electricity generation, the main areas where turbines are applied nowadays, even though aircraft now play a more important and quite more visible role than ships in what concerns transports.

Several improvements followed, along with some new creative designs, including a design by Nikola Tesla, the Tesla Turbine [4]. Around the 1950s designs were good enough to be manufactured industrially and continuously for several years, such as the Y100, an English Electric marine steam turbine, an example of a classical design that continued to be manufactured for more than 40 years after its creation [5]. More important for the aircraft industry though, was Sir Frank Whittle's patent for a turbojet engine in 1930 [6]. Before this breakthrough the gas turbine was actually not feasible for aircraft use, due to a too low power to weight ratio. Aircraft turbines followed an expected study and improvement along with the development of both military and commercial aircraft industries. In fact, when Whittle appeared stressed with the great simplicity of his engine, Hives, at the time director of Rolls Royce reportedly commented, "We'll soon design the bloody simplicity out of it."[7] (figure 1.1).

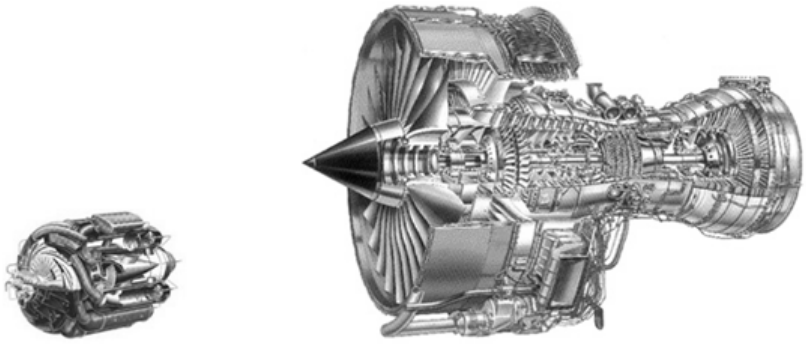

Figure 1.1: *The Whittle W-1 of 1941(left) and a modern Trent engine (right) [3]*

Nowadays, a mature understanding of the subject exists and it can be coded and applied into a computer program, such as the one we propose to accomplish here and which can be developed in order to obtain a preliminary design of a machine that powers most of the modern world.

Design is increasingly dependent on optimization tools. On the other hand, these optimization tools need a good input in order to reach an optimized design. Also, the better the input, the more constrained the design space may be, enabling a reduction in time and costs. Even though work has been accomplished when it comes to the optimization of a turbine design, the preliminary design phase is often worked out by hand. This results in a loss of time that the industry cannot accept when the demand for celerity and quality is so high. However, this kind of optimization, such as the one described in [8], will be the

ultimate end of the data output of the program hereby developed. The joining of these two parts should be able to deliver, by itself, a finished, optimized and feasible turbine design.

In what concerns the tools needed for the development of this program, they have all been quite well understood for a long time (as referred to before), with, for instance, Horlock[9] being one of the most used references for this document. In fact [9] and [10] contain the main theoretical basis for the design work here developed. All thermodynamic background for this document was taken from these last two references, along with [11] and [12]. However, in what concerns designer experience, such as "rules of thumb" and typical values not usually found in the literature, [13] was fundamental in the development of this design procedure. Besides that, [14] (with its respective figures improved by [15]) was the main reference for loss calculation, since it comprises a systematic and complete method for the loss calculation of both stator and rotor. Furthermore, [16], [17] and [18] were also used for the implementation of the secondary loss coefficient found in [14]. [9] and [19] were also taken as references for the loss calculation, but for Soderberg's loss model, a simpler approach to this type of calculation. This loss calculation method was only used at the 1D analysis. For the radial equilibrium theory, besides the already referred [10], [9] and [13], [20] was also taken as a reference for both the expressions and the methodologies used in radial equilibrium theory. Moreover, [21] and [22] were used for the sole purpose of the calculation of some geometric aspects of the turbine. For the airfoil calculation, reference [23] was used, being the only document of the kind, since it allows for a methodical and programmable method of calculating airfoil coordinates. Finally, [24], [25] and [26] are connected to the numerical implementation in C programming language of this design exercise.

1.4 Report Structure

Following this small introduction, the reader will find a general view of the design procedure, a road-map to the basic reasoning behind the preliminary design task ahead. After this, the theoretical background for the tools that shall be used in the report is presented. Then, each of the sections referred to in the design procedure will be explained in a series of chapters. These include all calculations necessary for implementing the theories presented before, such as MLA and RET. The contents of these chapters will be further explained in the design task chapter and in the chapters themselves.

Chapter 2

Design Procedure

This design task can be divided in six fundamental elements: the Engine Cycle Analysis, that regards the engine as a whole and takes each element of it as a "black-box"; the Mean Line Analysis, comprising the 1D design of the turbine that is the center of our study; the Design Control, with the purpose of checking the feasibility of the design; the ISRE, Isentropic Simple Radial Equilibrium, a more detailed, 2D analysis of the turbine; the NISRE, Non-Isentropic Simple Radial Equilibrium, which accounts with the losses in this 2D design; and finally the Airfoil Selection, which is based on the results from the NISRE and delivers a 3D geometry. The program structure is presented in figure 2.1 in a flow chart.

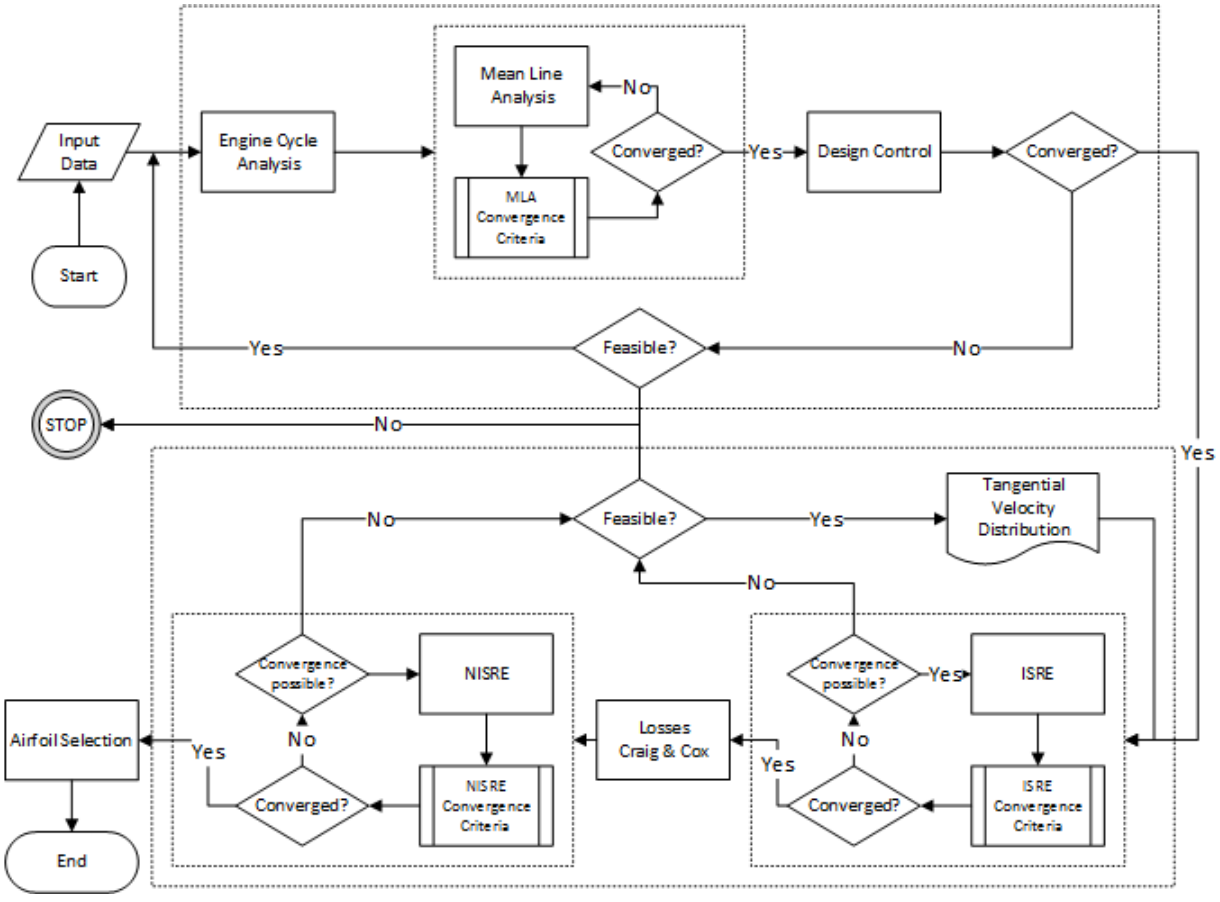

Figure 2.1: *Design Procedure*

Each of these design sections will be explained in detail in the following chapters, including the understanding of the theory behind them and the necessary implementation in the C code. Several convergence points that are presented throughout the flow chart shall also be explained. The loss calculation through the Soderberg's correlation is not shown in the flowchart for the sake of simplicity. It occurs inside the MLA block. There are several cases throughout the computation that lead to a STOP. This happens when the input data given by the user can't deliver a feasible design in any way. We also remark the existence of two main blocks, one comprising the ECA and MLA, corresponding to the 1D design, and the second comprising the Radial Equilibrium, corresponding to the 2D design.

2.1 Overview of 1D Design

In the 1D design, an engine study is first conducted, based on global engine variables. At the end of this analysis, the total temperatures and pressures at the beginning and end of the gas generator are known, along with the engine mass flow, quantity that passes down the program and that we must always ensure to be the same. The power that the gas generator must deliver is also found at this point of the calculation. The Mean Line Analysis provides a simple 1D design of a turbine, by basing all calculations at mean radius. The inputs are not only the information from the ECA, but also other inputs concerning the turbine itself, such as R_p, α_2, β_3 and U, all mean radius values. These values may change throughout the computation, due to the action of the design control function. Therefore, the MLA calculation provides the user with mean radius pressures, temperatures and velocity triangles. Associated to this calculation, the mean radius losses are calculated using Soderberg's correlation, which provides the blading efficiency for both stator and rotor. Since we can relate the blading efficiency of stator and rotor with the total to total efficiency of the gas generator, the ECA must be run again (since it depends on the gas generator total to total efficiency), until convergence. The variables R_p, α_2, β_3 and U can also be changed throughout the computation, until all design requirements are met. Every time the design control function acts, the 1D block must be recalculated, until convergence. Some of the geometry of the turbine is already calculated in the MLA, which enables us to, for example, check U^t, an important quantity since it must be controlled due to material constraints. Inside the MLA block itself, several convergences also occur, on p_1 (only a guess in the beginning), on each of the blading efficiencies and on M_3. The calculation should try to deliver an as low as possible M_3. In the extreme case that the several variables controlled by the design control function can't change anymore to accomplish the design requirements, the design is considered infeasible and the computation stops.

2.2 Overview of 2D Design

The output of the 1D design is the basis for starting the 2D design, at the ISRE block, along with a chosen tangential velocity distribution. The ISRE is a first approximation for the NISRE, in which we assume zero losses, along with choosing $\frac{dh_0}{dr} = 0$ (design choice that will be kept for the NISRE). The main objective of the ISRE calculation is to obtain a velocity distribution, based on the 1D results and

the imposed V_θ, that satisfies the mass flow value obtained in the ECA. The program varies the mean axial velocity (on which the overall distribution will depend) until satisfying this criteria. In case this is not possible, the program issues a warning and the user is asked to choose another tangential velocity distribution. On the other hand, if the program succeeds in satisfying the mass flow from the ECA, the new velocity radial distributions are computed, along with pressure and temperature distributions. All these data will be needed for the loss calculation with the Craig & and Cox[14] loss correlation. This loss calculation comprises three elements: profile loss, secondary loss and leakage loss. At the beginning of the loss calculation, the geometry is also calculated. This includes not only geometry at the mean radius, as before, but also the radial distributions of some quantities, such as stagger and throat size. The values of the loss and its radial distribution will allow for the calculation of $\frac{ds}{dr}$, term that was taken as zero for the ISRE calculation, but can now be computed and taken into account. A process in all similar to the one in the ISRE takes place, to find the new velocity distribution now accounting with the losses. This process is repeated several times, since the NISRE is an iterative process. Ensuring convergence is absolutely necessary in order to achieve reliable results. It may happen that a velocity distribution for which there was an ISRE solution, does not have a NISRE solution. In this case the user is asked to choose another tangential velocity distribution and the process restarts at the beginning of the 2D design, the ISRE. If, both in the ISRE and NISRE cases, no more tangential velocity distributions are available for use, the program stops due to the infeasibility of the design. However, if the NISRE indeed finds a new velocity distribution that satisfies the mass flow found in the ECA, the new radial distributions of quantities such as velocity, pressure and temperature are computed. The results of the NISRE will be the input for the airfoil selection that occurs in the end of this design exercise, with particular importance given to the velocity triangles, since this method is mainly based on the turning required for each blade.

Chapter 3

Theoretical Background

The theoretical basis for the work developed in this thesis is presented in this chapter. The information hereby displayed is a small compilation of the tools that will be used throughout the entire document. The information is presented with emphasis on final results rather than on the demonstration of the latter, since that is not the scope of this thesis. However, the availability of these results in this document is of utmost importance for understanding what is to follow.

3.1 Isentropic Flow

The notion of isentropic flow is very important for turbine design. Obviously, an increase in entropy will always be observed in real processes, since a gas turbine represents an irreversible process. However, by coupling the notion of efficiency with the mathematical expressions resulting from the notion of isentropic flow, we are able to model the real behaviour of our engine. For one-dimensional isentropic flow of a perfect gas through a duct of varying cross-section, we have four main equations: continuity, energy, perfect gas equation and the isentropic relation.

$$\text{Continuity: } \rho AV = constant \tag{3.1a}$$

$$\text{Energy: } h_0 = h + \frac{V^2}{2} \tag{3.1b}$$

$$\text{Perfect Gas Equation: } p = \rho RT \tag{3.1c}$$

$$\text{Isentropic relation: } \frac{p}{\rho^\kappa} = constant \tag{3.1d}$$

Equation 3.1b is written for the absolute velocity V. As it will be shown in section 3.5.3, we must also account with relative velocities W (due to the rotor rotation speed U). Hence, a relative total enthalpy must be defined.

$$\text{Energy: } h_0^r = h + \frac{W^2}{2} \tag{3.2}$$

The Mach number is defined as the ratio of the velocity V to the local speed of sound a:

$$M = \frac{V}{a} \tag{3.3}$$

with $a = \sqrt{\kappa RT}$.

Hence, using the Mach number definition, we may derive the following expressions:

$$\frac{p}{p_0} = \left(1 + \frac{\kappa - 1}{2} M^2\right)^{\frac{-\kappa}{\kappa - 1}} \tag{3.4}$$

$$\frac{T}{T_0} = \left(1 + \frac{\kappa - 1}{2} M^2\right)^{-1} \tag{3.5}$$

$$\frac{p_0}{p} = \left(\frac{T_0}{T}\right)^{\frac{\kappa}{\kappa - 1}} \tag{3.6}$$

3.2 Non-isentropic Flow

According to [12], the second law of thermodynamics states:

$$ds = \frac{dQ}{T} \tag{3.7}$$

Knowing that $dQ = dh_0 - V dp$ and $dh_0 = c_p dT$ we arrive at the final expression for the entropy change between two states:

$$\Delta s = c_p ln \left(\frac{T_{02}}{T_{01}}\right) - R \ln \left(\frac{p_{02}}{p_{01}}\right) \tag{3.8}$$

3.3 Sutherland's Law

Sutherland's Law was used in this document in order to calculate the dynamic viscosity. This law is expressed by:

$$\frac{\mu}{\mu_0} = \left(\frac{T}{T_0}\right)^{\frac{3}{2}} \frac{T_0 + S}{T + S} \tag{3.9}$$

with $\mu = 1.716 \times 10^{-5} \frac{kg}{m/s}$, $T_0 = 273.15K$ and $S = 110.4K$.

3.4 Engine Thermodynamics

Before the actual turbine design, a simple engine cycle analysis is performed. The components of the engine and important equations regarding their behaviour are now presented.

3.4.1 Compressor

The process that occurs in the compressor is an adiabatic non-isentropic compression. A typical T-s diagram of a compressor is presented in figure 3.1, as taken from reference [11].

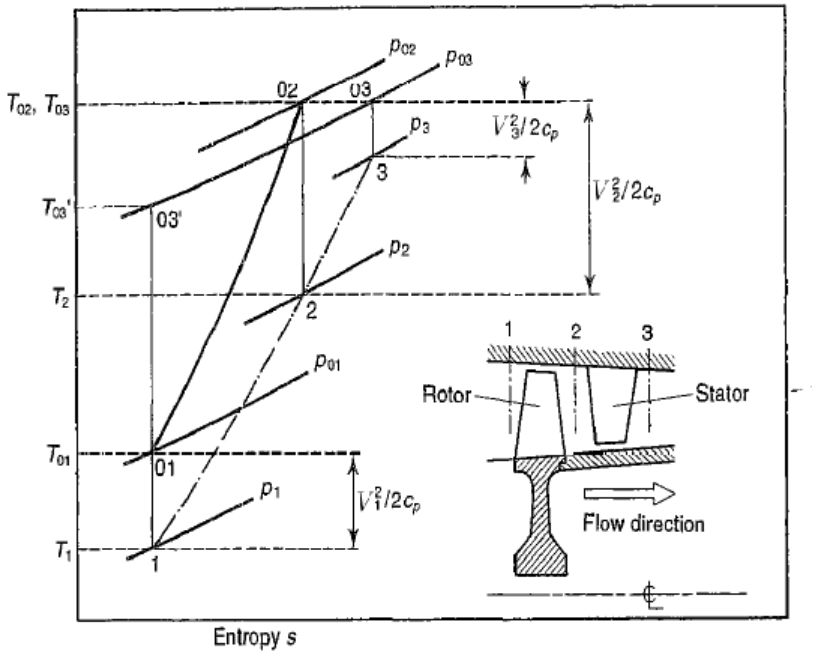

Figure 3.1: *Typical T-s diagram for a compressor*

According to the figure above, the power of the compressor is given by:

$$P_c = \dot{m}_{air} \left(h_{03} - h_{01}\right) = \dot{m}_{air} c_p \left(T_{03} - T_{01}\right) \tag{3.10}$$

Taking into account the non-isentropic quality of the process, the total pressure ratio and total temperature ratio at the beginning and end of the process can be related by the following equation, using the isentropic compressor efficiency.

$$\frac{T_{03}}{T_{01}} = 1 + \frac{1}{\eta_c} \left(\left(\frac{p_{03}}{p_{01}} \right)^{\frac{\kappa-1}{\kappa}} - 1 \right) \tag{3.11}$$

3.4.2 Combustion Chamber

The combustion chamber represents the heat addition section of the engine cycle. This process is described by a heat balance equation with basis on the first law of thermodynamics (in the following equation we take the subscripts 1 and 3 as representative of the inlet and outlet of the combustion chamber).

$$\dot{m}_f LHV \eta_{cc} = \left(\dot{m}_{air} + \dot{m}_f\right) C_{p_{gas}} \left(T_{03} - T_{01}\right) \tag{3.12}$$

Some pressure losses may occur in the combustion chamber. As such, a pressure ratio is defined to account for the losses in pressure $\left(\Pi_{cc} = \frac{p_{03}}{p_{01}}\right)$. This is different from the efficiency presented in the previous equation, that deals with fuel combustion related losses, rather than pressure losses.

3.4.3 Turbine

A complete h-s diagram, taken from reference [10], is presented in figure 3.2. This diagram will be used as a reference throughout the entire document for the design and analysis of the turbine.

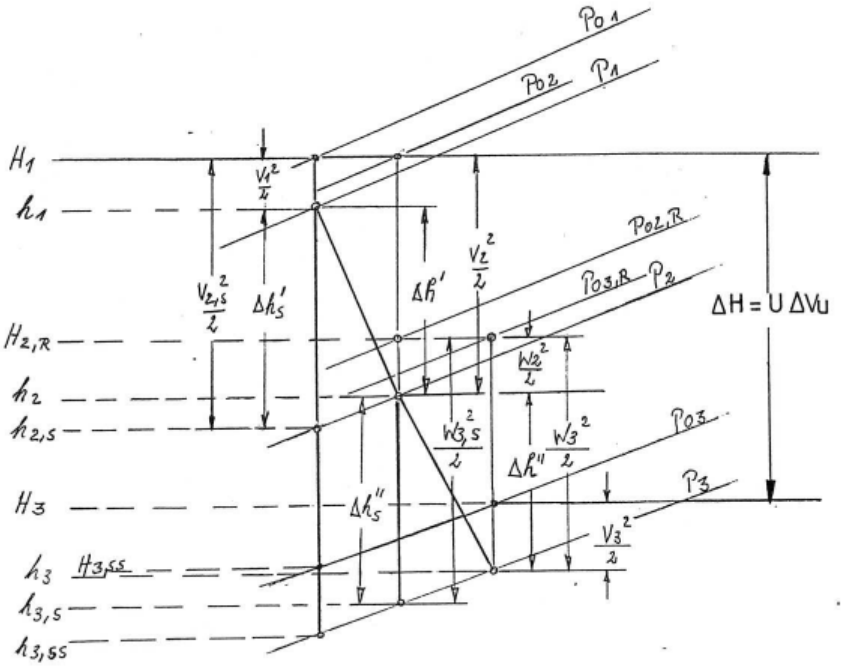

Figure 3.2: *Typical h-s diagram for a turbine*

As such, the power of the turbine is given by:

$$P_t = (\dot{m}_{air} + \dot{m}_f)\, c_p\, (T_{01} - T_{03}) \tag{3.13}$$

Taking into account the non-isentropic quality of the process, the total pressure ratio and total temperature ratio at the beginning and end of the process can be related by the following equation, using the isentropic compressor efficiency.

$$\frac{p_{03}}{p_{01}} = \left(1 - \frac{1}{\eta_{gg}} \left(1 - \frac{T_{03}}{T_{01}}\right)\right)^{\frac{\kappa_{gas}}{\kappa_{gas}-1}} \tag{3.14}$$

The equations that here describe the turbine are to be used only in the engine cycle analysis, where the turbine is taken (along with all other components of the engine) as a "black-box". Obviously, further turbine analysis theory must be applied in other to achieve an actual turbine design.

3.5 Turbine Aerothermodynamics

In this section we recover the typical h-s diagram of a turbine from figure 3.2, as a reference to understand turbine aerothermodynamics.

The conservation of mass flow and the fact that the process is adiabatic will be the two main guide lines for the computation of the mean line analysis. The latter is twofold, since the result of this assumption has an important difference whether it refers to the stator or the rotor. The different definitions of efficiency to be used in this document are also discussed.

3.5.1 Turbine Geometry

An axial-radial cut of a turbine, as presented in figure 3.3 (adapted from reference [10]), is the main reference for the purpose of turbine geometry analysis.

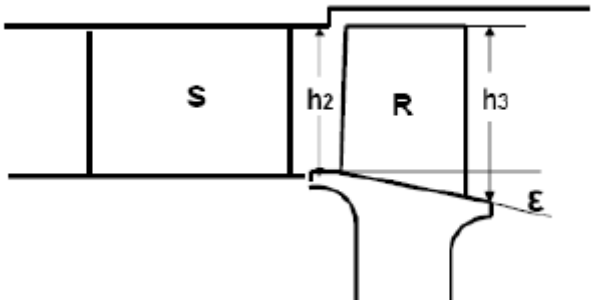

Figure 3.3: *Typical stage geometry in an unshrouded turbine*

S represents the stator and R the rotor. h_2 represents the height of section 2, that is, the difference between tip and hub radii of the stator exit, whilst h_3 does the same for section 3 (rotor exit). ϵ is the wall angle, defined by

$$\epsilon = \arctan\left(\frac{h_3 - h_2}{c_{x_R}}\right) \tag{3.15}$$

where c_{x_R} is the axial chord of the rotor, which shall be discussed promptly.

We may also have two wall angles, one at the hub and one at the tip. As shall be seen later, this document offers two design possibilities in what concerns rotor geometry: either the tip radius remains constant, as in figure 3.3, or the mean line radius remains constant, as in figure 3.4.

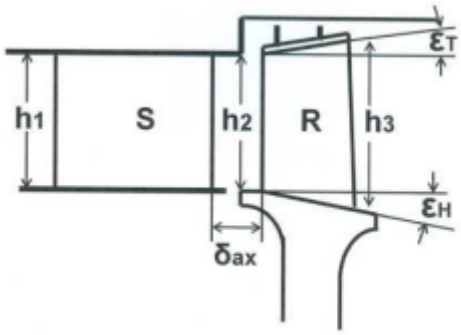

Figure 3.4: *Typical stage geometry in a shrouded turbine*

3.5.2 Blade Geometry

The following figures 3.5 and 3.6 represent the most important geometric definitions of the blade geometry parameters. These were adapted from [10] and [14] respectively.

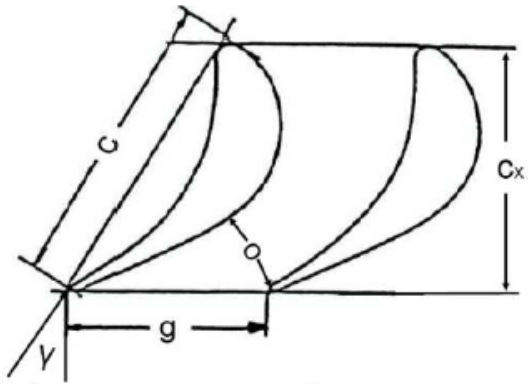

Figure 3.5: *Blade geometry [10]*

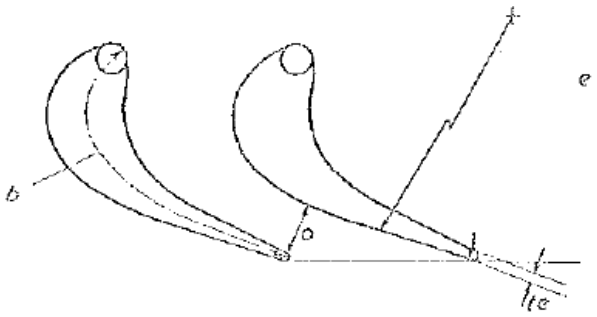

Figure 3.6: *Blade geometry [14]*

c is the chord, c_x is the axial chord, g is the pitch, o is the throat, γ is the stagger angle, e is the back surface radius, b is the backbone length and t_e is the trailing edge thickness.

3.5.3 Turbine Velocity Triangles

Figure 3.7 (as taken from [9]) represents the typical velocity triangles in a turbine.

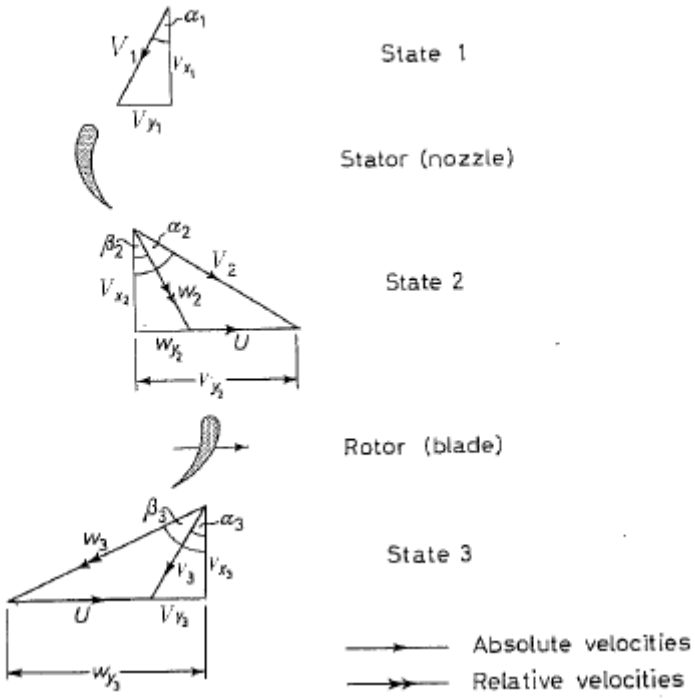

Figure 3.7: *Typical velocity triangles in a turbine stage*

From this figure we can write the following equations:

$$\vec{W}_2 + \vec{U}_2 = \vec{V}_2 \tag{3.16a}$$

$$\vec{W}_3 + \vec{U}_3 = \vec{V}_3 \tag{3.16b}$$

$$V_2 \cos(\alpha_2) = W_2 \cos(\beta_2) \tag{3.17a}$$

$$V_2 \sin(\alpha_2) = U + W_2 \sin(\beta_2) \tag{3.17b}$$

$$V_3 \cos(\alpha_3) = W_3 \cos(\beta_3) \tag{3.17c}$$

$$V_3 \sin(\alpha_3) = U + W_3 \sin(\beta_3) \tag{3.17d}$$

It is important to refer the different conventions regarding angles and velocities. First, there are different conventions as to whether the angles should be measured from the axial line or the meridional line. Henceforth, these conventions shall be referred to as English and German conventions, respectively. This document takes the English convention as default. However, due to the different references used throughout the document, there may be a need to use the German convention at certain sections of this thesis. In these situations, the reader will be informed. The second convention to be discussed regards which is the positive direction of the meridional axis of the reference frame. In this document, and along with the figure above from [9], absolute and relative angles, along with tangential velocities, are measured as positive in the direction of rotation when downstream of the stator. Downstream of the rotor, these quantities are measured as positive against the direction of rotation. However, in many documents, absolute and relative angles, along with tangential velocities, are measured as positive in the direction of rotation when downstream of the rotor. When needed be, the convention may be changed in order to use certain references. Again, the reader will be warned if such is the case.

3.5.4 Turning Angle

The turning angle is defined as the sum of the relative inlet and outlet angles of each turbine component. As such, for the stator we have,

$$\Delta\alpha_S = \alpha_1 + \alpha_2 \tag{3.18}$$

whilst for the rotor we have

$$\Delta\alpha_R = \beta_2 + \beta_3 \tag{3.19}$$

3.5.5 Conservation of mass flow

Regarding the conservation of mass flow we can simply write:

$$\dot{m} = \rho_1 A_1 V_{1_x} = \rho_2 A_2 V_{2_x} = \rho_3 A_3 V_{3_x} \tag{3.20}$$

3.5.6 Adiabatic Flow

When referring to the stator, this simply implies the conservation of total enthalpy, or, since this document always assumes constant c_p, conservation of total temperature. This results in:

$$T_1 + \frac{V_1^2}{2c_p} = T_2 + \frac{V_2^2}{2c_p} \tag{3.21}$$

The rotor, however, is a different case, since we must take rotation into account. If we look into the definition of energy and angular momentum for the turbine we have, respectively:

$$\dot{W} = \dot{m}\,(h_{01} - h_{03}) \tag{3.22}$$

$$M = \dot{m}\,(r_1 V_{1_\theta} - r_3 V_{3_\theta}) \tag{3.23}$$

Since we have,

$$\dot{W} = M\Omega \tag{3.24}$$

We arrive at

$$h_{01} - h_{03} = \Omega\,(r_1 V_{1_\theta} - r_3 V_{3_\theta}) \tag{3.25}$$

From this, we can rearrange the equation into Euler's equation for turbomachinery

$$h_{01} - U_1 V_{1_\theta} = h_{03} - U_3 V_{3_\theta} \tag{3.26}$$

We hence arrive at the definition of rothalpy, represented by the letter I,

$$I = h_0 - U V_\theta \tag{3.27}$$

The conservation of rothalpy is used when regarding the rotor. However, we can observe that when applying the definition to the stator, we have $U = 0$ and hence $I = h_0$, so arriving at the exact same result.

In order to arrive at an easier to use equation, we further use the velocity triangle relations, getting:

$$h + \frac{W^2}{2} - \frac{U^2}{2} = const. \tag{3.28}$$

Given that c_p is assumed constant, we can write the actual mathematical expression used in this document:

$$T_2 + \frac{W_2^2}{2c_p} - \frac{U_2^2}{2c_p} = T_3 + \frac{W_3^2}{2c_p} - \frac{U_3^2}{2c_p} \tag{3.29}$$

3.5.7 Design Parameters

The three main so-called Design Parameters will be presented in this section. The degree of reaction, flow coefficient and load coefficient, even if not used as a starting point for design, are always good references for checking a final or preliminary design of a turbine.

Degree of Reaction

The degree of reaction is a quantity that represents the amount of contribution of the rotor for the static pressure rise in the stage. According to [10], and taking into account figure 3.2, the degree of reaction is defined by:

$$R_h = \frac{\Delta h''}{\Delta h' + \Delta h''} \tag{3.30}$$

This is also called the enthalpy degree of reaction, since, for simplicity, a designer often uses a pressure degree of reaction, defined by:

$$R_p = \frac{\Delta p''}{\Delta p' + \Delta p''} \tag{3.31}$$

Flow Coefficient

The flow coefficient is given by the ratio between axial velocity and rotation speed.

$$\phi = \frac{V_x}{U} \tag{3.32}$$

Load Coefficient

The loading coefficient is defined as the ratio between change in total enthalpy and the square of the rotation speed.

$$\psi = \frac{\Delta h_0}{U^2} \tag{3.33}$$

In fact, we can write this as:

$$\psi = \frac{c_p \left(T_{01} - T_{03}\right)}{U^2} \tag{3.34}$$

3.5.8 Turbine Efficiency

Stage Efficiency

There are two ways of expressing stage efficiency, the total to total efficiency, used in this document as the main reference, and the total to static efficiency. These are given by the following equations, respectively.

$$\eta_{TT} = \frac{h_{01} - h_{03}}{h_{01} - h_{03_{ss}}} \tag{3.35}$$

$$\eta_{TS} = \frac{h_{01} - h_{03}}{h_{01} - h_{3_{ss}}} \tag{3.36}$$

Since we have a constant c_p, we can write these equations as:

$$\eta_{TT} = \frac{T_{01} - T_{03}}{T_{01} - T_{03_{ss}}} = \frac{T_{01} - T_{03}}{T_{01} - \left(T_{3_{ss}} + \frac{V_{3_{ss}}^2}{2c_p}\right)} \tag{3.37}$$

$$\eta_{TS} = \frac{T_{01} - T_{03}}{T_{01} - T_{3_{ss}}} \tag{3.38}$$

where $T_{03_{ss}}$ and $T_{3_{ss}}$ are given by (figure 3.2):

$$T_{03_{ss}} = T_{01} \left(\frac{p_{03}}{p_{01}}\right)^{\frac{k-1}{k}} \tag{3.39}$$

$$T_{3_{ss}} = T_{01} \left(\frac{p_3}{p_{01}}\right)^{\frac{k-1}{k}} \tag{3.40}$$

Blading efficiency

The isentropic blading efficiency definition used as a main reference is, in the stator case:

$$\eta = \frac{h_{01} - h_2}{h_{01} - h_{2_s}} = \frac{T_{01} - T_2}{T_{01} - T_{2_s}} = \frac{V_2^2}{V_{2_s}^2} \tag{3.41}$$

For the rotor we have:

$$\eta = \frac{h_{02}^r - h_3}{h_{02}^r - h_{3_s}} = \frac{T_{02}^r - T_3}{T_{02}^r - T_{3_s}} = \frac{W_3^2}{W_{3_s}^2} \tag{3.42}$$

The loss in kinetic energy is defined as:

$$\zeta = \frac{V_{2_s}^2 - V_2^2}{V_{2_s}^2} \tag{3.43}$$

or, as in the fashion more commonly used in this document, as referred to V_2^2 instead of $V_{2_s}^2$:

$$\xi = \frac{V_{2_s}^2 - V_2^2}{V_2^2} \tag{3.44}$$

For the rotor the expressions are similar but using the exit velocity relative to the rotor, W_3.

These 3 definitions can be interchangeably related by:

$$\eta = 1 - \zeta \tag{3.45a}$$

$$\eta = \frac{1}{1 + \xi} \tag{3.45b}$$

$$\xi = \frac{\zeta}{1 - \zeta} \tag{3.45c}$$

3.6 Radial Equilibrium Theory

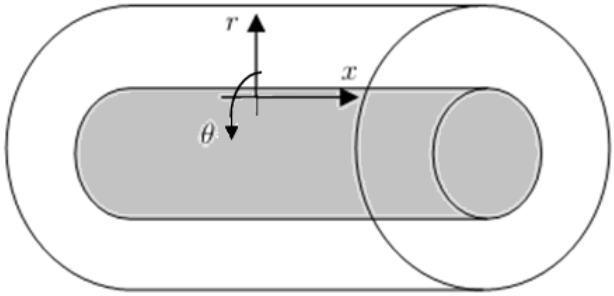

Figure 3.8: *Reference frame used in radial equilibrium theory*

On figure 3.8, we can observe the reference frame used in RET. The cylinder in grey represents the hub radius, whilst the clear cylinder represents the tip radius.

In RET we assume that the flow is axisymmetric, the blade rows do not interact and there are no side forces. The basic assumption of radial equilibrium theory is that the radial velocity is zero, $V_r = 0$. Taking the momentum equations of the turbine, according to [9],

$$\text{Radial:} \quad -\frac{1}{\rho}\frac{\partial p}{\partial r} = V_x \frac{\partial V_r}{\partial x} + V_r \frac{\partial V_r}{\partial r} - \frac{V_\theta^2}{r} \tag{3.46a}$$

$$\text{Meridional:} \quad 0 = V_x \frac{\partial V_\theta}{\partial x} + V_r \frac{\partial V_\theta}{\partial r} + \frac{V_r V_\theta}{r} \tag{3.46b}$$

$$\text{Axial:} \quad -\frac{1}{\rho}\frac{\partial p}{\partial x} = V_x \frac{\partial V_x}{\partial x} + V_r \frac{\partial V_x}{\partial r} \tag{3.46c}$$

With $V_r = 0$, the radial momentum equation becomes,

$$\frac{1}{\rho}\frac{\partial p}{\partial r} = \frac{V_\theta^2}{r} \tag{3.47}$$

If we now take the definition of stagnation enthalpy and then apply $V_r = 0$, we get the following:

$$h_0 = h + \frac{V^2}{2} \tag{3.48}$$

$$h_0 = h + \frac{V_\theta^2}{2} + \frac{V_x^2}{2} + \frac{V_r^2}{2} \tag{3.49}$$

$$h_0 = h + \frac{V_\theta^2}{2} + \frac{V_x^2}{2} \tag{3.50}$$

According to [9], the Gibb's relation as derived from the second law of Thermodynamics is given by:

$$Tds = dh - \frac{1}{\rho}dp \tag{3.51}$$

Using 3.47, 3.50 and 3.51 we arrive at

$$\frac{dh_0}{dr} - \frac{Tds}{dr} = \frac{V_\theta^2}{r} + V_\theta \frac{dV_\theta}{dr} + V_x \frac{dV_x}{dr} \tag{3.52}$$

For a design exercise one usually takes the total enthalpy as constant, as it has been done in this document. A more practical way of working with equation 3.52 is presented below. This form of the equation shall be used for the ISRE and NISRE computations.

$$\frac{V_\theta}{r}\frac{d\left(rV_\theta\right)}{dr} + V_x \frac{dV_x}{dr} + T\frac{ds}{dr} = 0 \tag{3.53}$$

3.7 Numerical integration and differentiation

When numerical integration was necessary, the trapezium rule, presented below, was used. According to [24], this integration scheme is second order accurate and expressed by the general formula below.

$$\int_a^b f(x)dx \approx (b-a)\left[\frac{f(a)+f(b)}{2}\right] \tag{3.54}$$

Finite differences were used for numerical differentiation. Fourth order accurate finite differences were applied in RET, whilst second order accurate finite differences were used in the airfoil selection process, due to the limitations imposed by the non-uniformity of the points spacing (table 8.1). The formulas presented below can easily be demonstrated using Taylor series. Three different finite differences formulas were used: central, backward and forward differences. According to [25], the fourth order finite differences can be expressed in the following fashion for a general variable u with uniform grid spacing Δx:

$$\text{Central difference: } \frac{\partial u}{\partial x} = \frac{u_{i-2} - 8u_{i-1} + 8u_{i+1} - u_{i+2}}{12\Delta x} \tag{3.55a}$$

$$\text{Backward difference: } \frac{\partial u}{\partial x} = \frac{25u_{i-4} - 48u_{i-3} + 36u_{i-2} - 16u_{i-1} + 3u_i}{12\Delta x} \tag{3.55b}$$

$$\text{Forward difference: } \frac{\partial u}{\partial x} = \frac{-25u_i + 48u_{i+1} - 36u_{i+2} + 16u_{i+3} - 3u_{i+4}}{12\Delta x} \tag{3.55c}$$

On the other hand, second order finite differences are given by:

$$\text{Central difference: } \frac{\partial u}{\partial x} = \frac{u_{i+1} - u_{i-1}}{2\Delta x} \tag{3.56a}$$

$$\text{Backward difference: } \frac{\partial u}{\partial x} = \frac{u_{i-2} - 4u_{i-1} + 3u_i}{2\Delta x} \tag{3.56b}$$

$$\text{Forward difference: } \frac{\partial u}{\partial x} = \frac{-3u_i + 4u_{i+1} - u_{i+2}}{2\Delta x} \tag{3.56c}$$

Chapter 4

Engine Cycle Analysis

4.1 Engine Architecture

The considered engine is a turboshaft engine, comprising a propeller driven by a turbine which shall be mentioned to as power turbine; a compressor driven by another turbine which will be referred to as gas generator (and it is the object of our study) and a combustion chamber. Figure 4.1 shows a schematic view of the engine and its components, as well as the numbering adopted in order to analyse the engine cycle.

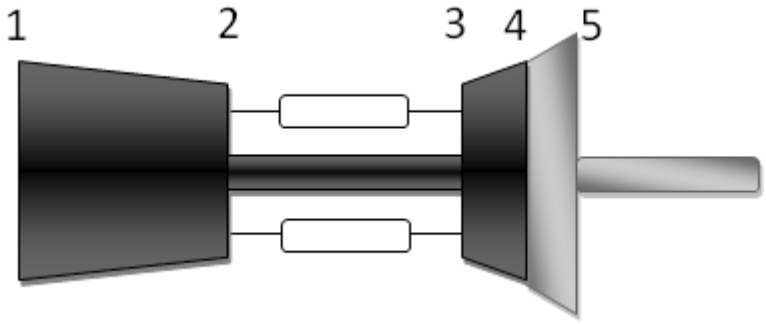

Figure 4.1: *Engine Scheme*

4.2 Global Starting Data

Since the objective is to obtain a general procedure for turbine design starting from global data, selecting which data the user is required to input is a very important step for the development of this methodology. It is observable that several scalars are required as the global starting data. These are: the total pressure at the beginning and end of the cycle, the inlet total temperature, the turbine inlet total temperature, the power required for the power turbine, the pressure ratio achievable by the compressor and the heat capacity ratio and heat capacity at constant pressure for the flows before and after the combustion chamber. Guesses concerning efficiencies of the components, Π_{cc} and LHV are also needed.

4.3 Calculation Procedure

The equations here described are based on the ones shown in section 3.4, but with a specific order of calculation for each quantity. We note that η_{gg} (the total to total efficiency η_{TT} of the turbine being designed) is, in the first iteration, just a user guess, but shall change according to Soderberg's loss correlation, as it will be explained later. The main scalars from this ECA analysis that shall be used afterwards are the total temperatures and pressures and the engine mass flow.

Compressor

The total temperature at section 2 is given by:

$$T_{02} = T_{01}\left(1 + \frac{1}{\eta_c}\left(\Pi_c^{\frac{\kappa_{air}-1}{\kappa_{air}}} - 1\right)\right) \tag{4.1}$$

The total pressure at section 2 is given by:

$$\frac{p_{02}}{p_{01}} = \Pi_c \tag{4.2}$$

The power per unit of air mass flow in the compressor is given by:

$$\frac{P_c}{\dot{m}_{air}} = C_{p_{air}}\left(T_{02} - T_{01}\right) \tag{4.3}$$

Combustion Chamber

The total pressure ratio in the combustion chamber is given by:

$$\frac{p_{03}}{p_{02}} = \Pi_{cc} \tag{4.4}$$

The heat balance in the combustion chamber is given by:

$$\dot{m}_f LHV \eta_{cc} = \left(\dot{m}_{air} + \dot{m}_f\right) C_{p_{gas}}\left(T_{03} - T_{02}\right) \tag{4.5}$$

This enables us to find the ratio $\frac{\dot{m}_f}{\dot{m}_{air}}$.

Gas Generator

Since the gas generator drives the compressor, we can relate the power between the two, taking into account the mechanical efficiency, using:

$$\frac{P_{gg}}{\dot{m}_{air}}\eta_m = \frac{P_c}{\dot{m}_{air}} \tag{4.6}$$

As such, we can find the temperature T_{04} using,

$$\frac{P_{gg}}{\dot{m}_{air}} = \left(1 + \frac{\dot{m}_f}{\dot{m}_{air}}\right) C_{p_{gas}}\left(T_{03} - T_{04}\right) \tag{4.7}$$

The total pressure ratio can be related to the total temperature ratio through:

$$\frac{p_{04}}{p_{03}} = \left(1 - \frac{1}{\eta_{gg}}\left(1 - \frac{T_{04}}{T_{03}}\right)\right)^{\frac{\kappa_{gas}}{\kappa_{gas}-1}} \tag{4.8}$$

Enabling the calculation of p_{04}.

Power Turbine

The total pressure ratio of the power turbine can be related to the total temperature ratio using the following equation, necessary to compute T_{05}.

$$\frac{p_{05}}{p_{04}} = \left(1 - \frac{1}{\eta_{pt}}\left(1 - \frac{T_{05}}{T_{04}}\right)\right)^{\frac{\kappa_{gas}}{\kappa_{gas}-1}} \tag{4.9}$$

Mass flow and Power of the Components

Since we know the required power for the power turbine, we may use the expression for the turbine power to determine the air mass flow.

$$P_{pt} = \dot{m}_{air}\left(1 + \frac{\dot{m}_f}{\dot{m}_{air}}\right) C_{p_{gas}} \left(T_{04} - T_{05}\right) \tag{4.10}$$

It immediately follows:

$$\dot{m}_f = \frac{\dot{m}_f}{\dot{m}_{air}}\dot{m}_{air} \tag{4.11}$$

$$P_{gg} = \frac{P_{gg}}{\dot{m}_{air}}\dot{m}_{air} \tag{4.12}$$

$$P_c = \frac{P_c}{\dot{m}_{air}}\dot{m}_{air} \tag{4.13}$$

Chapter 5

Mean Line Analysis

As a first approach to the actual turbine design we use the mean line analysis, a 1D approach. In this analysis, an imaginary blade-to-blade plane, tangential at the mean radius is analysed and considered representative of the rest of the turbine. By applying this approximation, we are able to obtain an averaged analysis of the turbine, therefore allowing a basis to start more complex analysis. The mean line analysis computes not only the properties of the flow, pressure, temperature, Mach number, but also the velocity triangles of the turbine at mean radius. In fact, losses are also considered, with focus on the efficiencies of the stator and rotor (for now guessed values that must be checked in the end and iterated on). In this section all considerations regarding this first analysis will be discussed, from the assumptions made to the calculation procedure, going through the method of loss calculation.

5.1 Assumptions

In the mean line analysis, we consider the mean radius blade-to-blade plane to be representative of the turbine. This is very reasonable for stages where hub and tip speeds are very similar. In any case, a 3D analysis must follow, in order to account for three-dimensional effects.

5.2 Losses

5.2.1 Previous Considerations

Some aspects of the turbine geometry must be computed before starting the loss calculation. We must note that the loss calculation occurs at the end of each MLA iteration, when certain quantities are already known, enabling us to calculate the geometry figures that are to follow.

Radii

The hub and tip radii for both sections 2 and 3 must be calculated. For this, a ratio of hub to tip radii had to be assumed, based on historic trends. As such, we typically assume (this can be changed by the user):

$$\frac{r_2^h}{r_2^t} = 0.9 \tag{5.1}$$

Taking the mass flow rate equation for section 2, we have:

$$\dot{m} = \rho_2 A_2 V_{2_x} \tag{5.2}$$

Since the area is given by $A_2 = \pi \left({r_2^t}^2 - {r_2^h}^2 \right)$, we can write:

$$\dot{m} = \rho_2 V_{2_x} \pi \left({r_2^t}^2 - {r_2^h}^2 \right) \tag{5.3}$$

$$\dot{m} = \rho_2 V_{2_x} \pi {r_2^t}^2 \left(1 - \left(\frac{r_2^h}{r_2^t} \right)^2 \right) \tag{5.4}$$

Since we have the mass flow rate from the engine cycle analysis, ρ_2 and V_{2x} from the mean line analysis and we assumed $\frac{r_2^h}{r_2^t}$, we can now compute r_2^t and consequently r_2^h.

We can now calculate the radius of hub and tip at section 3. Two possibilities are available for the user: to keep the tip radius constant, or to keep the mean radius constant. By keeping the tip radius constant ($r_3^t = r_2^t$), we can immediately compute r_3^h using the mass flow rate equation for section 3.

$$\dot{m} = \rho_3 V_{3_x} \pi \left({r_3^t}^2 - {r_3^h}^2 \right) \tag{5.5}$$

As for keeping the mean radius constant, we know that,

$$r_3^m = r_2^m = \frac{r_3^h + r_3^t}{2} \tag{5.6}$$

Hence, we can write the section 3 tip radius as a function of the mean radius of section 2 and the hub radius of section 3.

$$r_3^t = 2r_2^m - r_3^h \tag{5.7}$$

Substituting in the mass flow equation for section 3, we get:

$$\dot{m} = \rho_3 V_{3_x} 4\pi r_2^m \left(r_2^m - r_3^h \right) \tag{5.8}$$

Through the previous equation we can compute r_3^h.

Chord

The chord is taken as constant from hub to tip, and it's calculated using the height of the blade and typical height to chord ratios. For the stator we typically have $\frac{h}{c} = 0.5 \rightarrow 0.8$ and for the rotor $\frac{h}{c} = 1.1 \rightarrow 1.5$. The values of 0.65 and 1.15 are assumed by the program. However, these values may be changed by the user. The chord of vane and blade are then calculated using the radii previously computed. However, it's important to notice that while in the stator there is no area change, the blade heights at inlet and outlet of the rotor are different. As such, a mean value for the height of the blade is taken to calculate the chord.

Plots

Several plots are used throughout this computation. These are mainly taken from references [9] and [21]. When choosing which of the graphs of a carpet plot should be used for calculation, it is more than likely that the desired number is not perfectly correspondent to one graph, but it is rather located between two. As such, both graphs are analysed and a linear interpolation is made in order to calculate the wished result. However, if a carpet plot value which is needed to choose a graph is above or below the values presented, the largest value graph or the smallest value graph is used. In these two cases, a warning is issued. Each graph is described by two columns of points, obtained directly from the papers through a digitizer program. When trying to find a specific value between two points, a linear interpolation is also used. For values larger or smaller than those presented with the x-axis, the last and first values, respectively, are used, issuing warnings. This last situation in particular is not recommended, since the value may be quite away from the plot domain, a possible sign that such a design is not feasible. In the warnings issued, both values for the x coordinate (the plot limit and the value on the calculation) are shown. This enables the user to assess if such an approximation is acceptable for each case. Every time plots are needed for any computation, they will be treated and used in the exact same way as explained here.

Stagger

The stagger angle prediction is based on the figure below from [22].

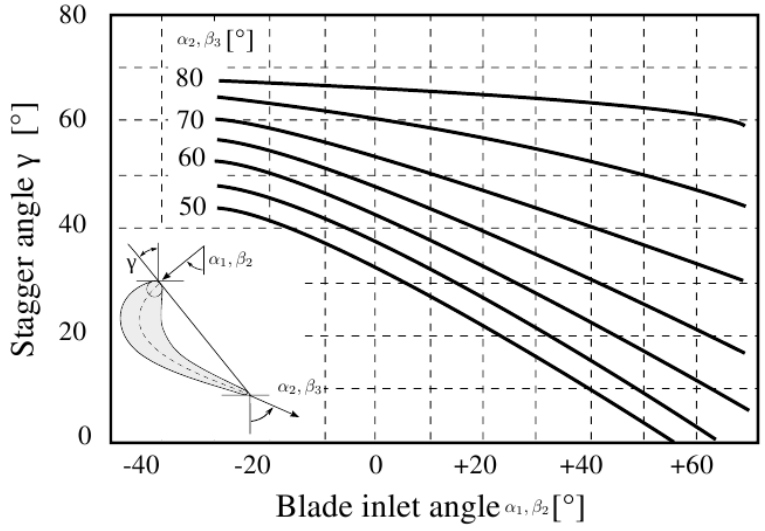

Figure 5.1: *Stagger angle for typical gas turbine blade sections [15]*

The inlet and outlet angles of either stator or rotor are the only figures needed for computing the stagger from figure 5.1.

Trailing Edge Thickness

The trailing edge thickness is also assumed constant throughout the radius. It is important to refer that two types of trailing edges have to be considered: uncooled and cooled. An uncooled trailing edge may

be as small as mechanically possible, that is, around 0.5 mm; a cooled blade demands a larger trailing edge thickness, around 1.2 mm. A cooled blade is implemented only if the temperature of the flow so demands. If however, the increased trailing edge thickness size is unreasonable when compared to other geometric parameters such as the chord and the pitch, a new trailing edge thickness is assumed and a new cooling method must be applied (with the program issuing a warning if such is the case). The trailing edge thickness is intricately connected with the pitch to chord ratio and consequently to the number of blades. Whatever the demand of the correlations used, a fixed trailing edge thickness of 0.5mm or 1.2mm is always preferred over, when possible. If so necessary, trailing edge thicknesses below 0.5mm are possible down to a minimum limit of 0.4mm. The method for the calculation of this parameter is presented in the following section for the determination of the number of blades.

Number of Blades

The number of blades is first calculated using mean line analysis values. We now present the flowchart (figure 5.2) for the calculation of the number of blades, pitch to chord ratio and trailing edge thickness.

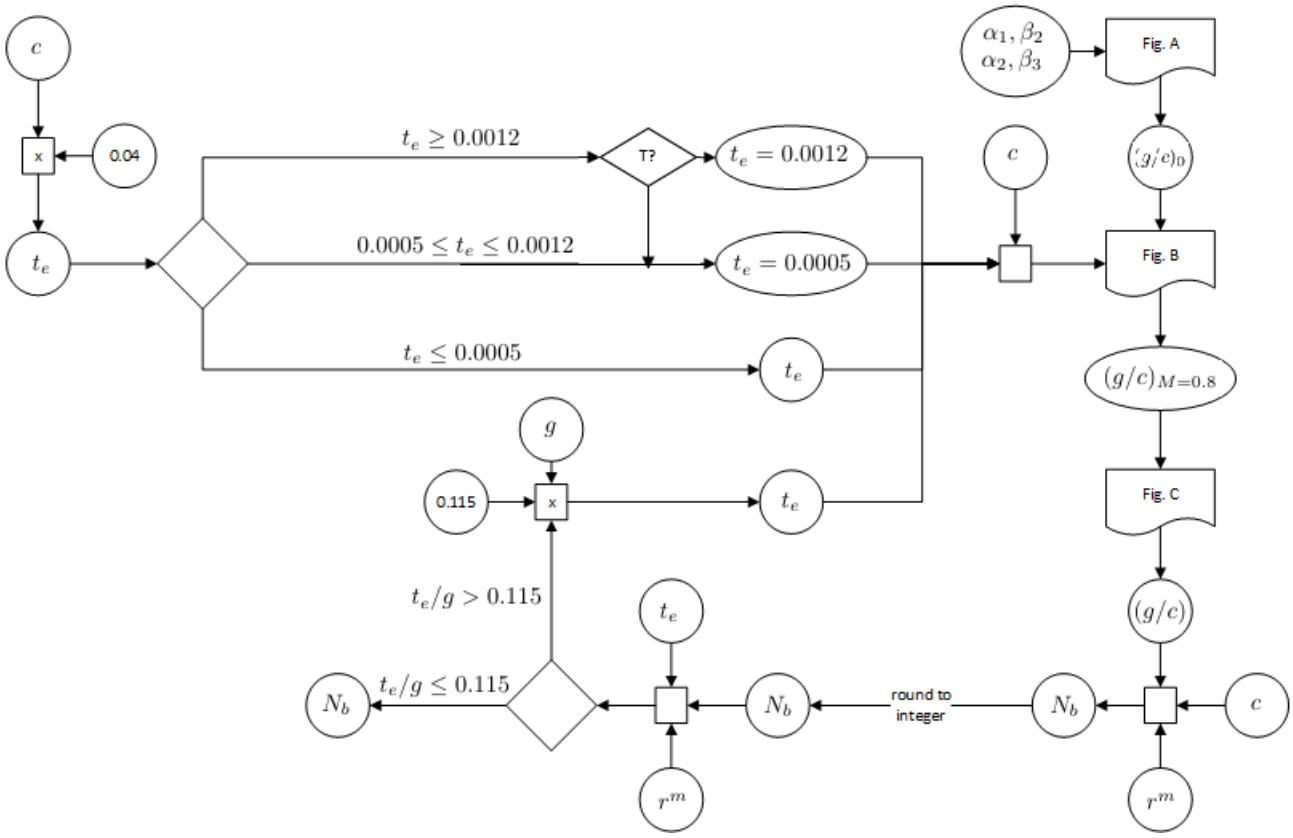

Figure 5.2: *Flow chart for the calculation of the number of blades*

The flow chart starts by determining the pitch to chord ratio. For this, reference [21] was used. This approach is composed of three plots. The first (figure 5.3) relates inlet and outlet angle in order to calculate $\left(\frac{g}{c}\right)_0$. This is a first value for the pitch to chord ratio, without the corrections for the trailing edge thickness and Mach number.

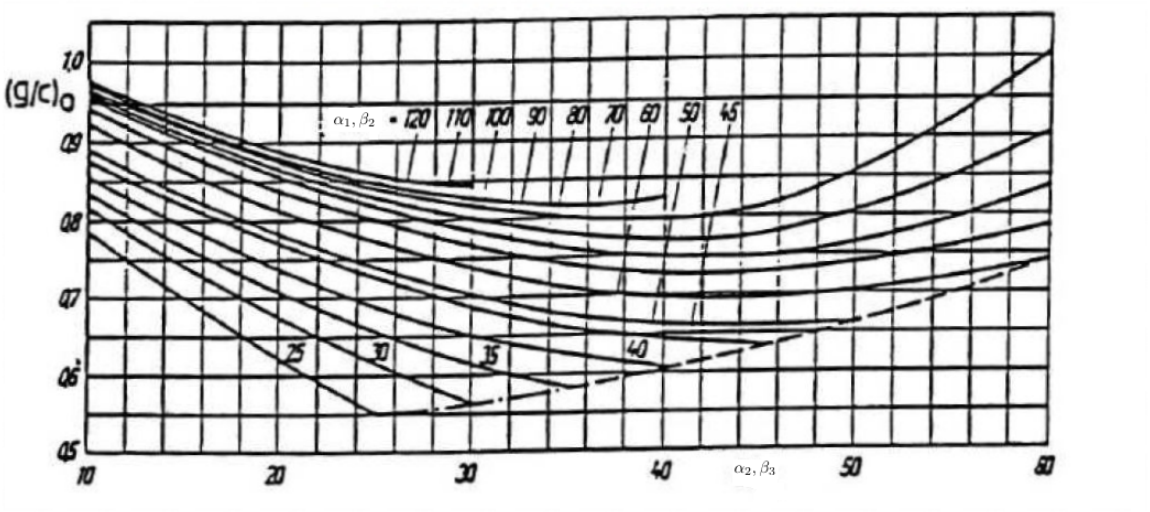

Figure 5.3: *Optimum pitch to chord ratios at zero trailing edge thickness (Fig. A)*

The second plot (figure 5.4) corresponds to the trailing edge thickness correction.

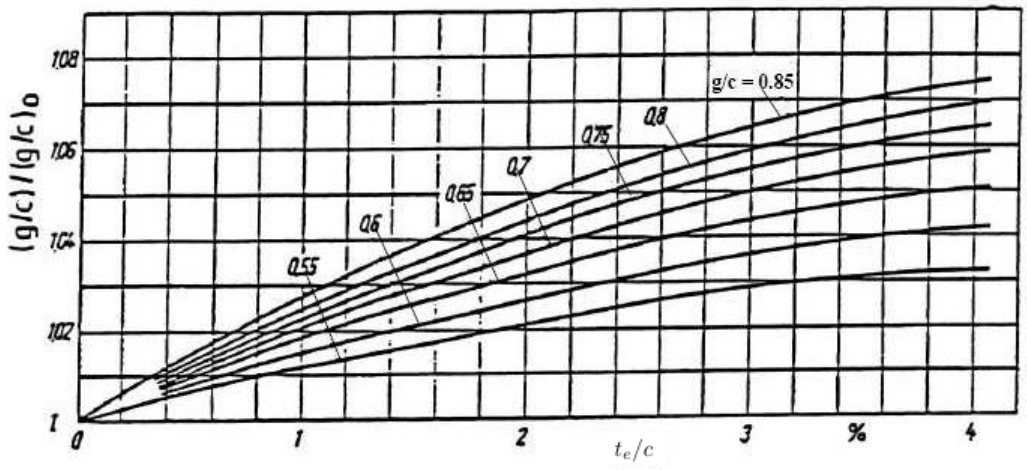

Figure 5.4: *Optimum pitch to chord ratios at non-zero trailing edge thickness (Fig. B)*

As it is possible to observe in the plot, a $\frac{t_e}{c} > 4\%$ is not even considered, due to the large losses that would produce. This is the reason why, for the first calculation of the trailing edge thickness, a first minimum limit is computed $t_e = 0.04c$. If cooling is necessary and the previously computed trailing edge thickness is above the limit for this case $t_e = 1.2mm$, a fixed trailing edge of $t_e = 1.2mm$ is used from here on, unless any further change is necessary. In the case, though, that the trailing edge thickness is below $t_e = 1.2mm$ but above $t_e = 0.5mm$, a thickness of 0.5 mm is used, for a cooled trailing edge is no longer possible anyway, and there is no reason to spoil the aerodynamics of the airfoil with a larger thickness. However, if this blade does indeed need cooling, the program issues a warning for the necessity of a different type of cooling system. With the tailing edge computed, $\frac{\left(\frac{g}{c}\right)}{\left(\frac{g}{c}\right)_0}$ may now be calculated. The last correction concerns the outlet Mach number (figure 5.5). After this, the value of $\frac{g}{c}$ is finally computed using the equation given after the plot.

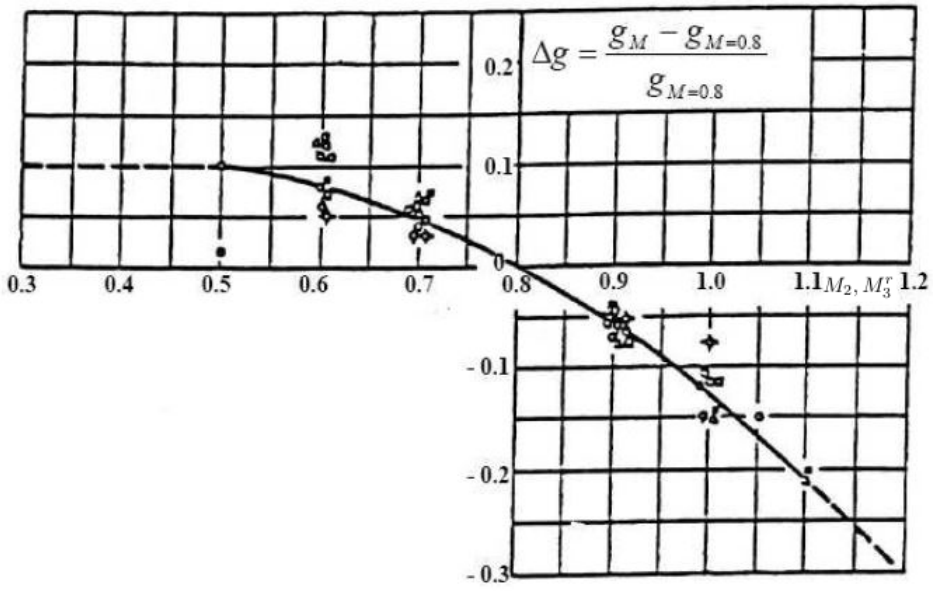

Figure 5.5: *Influence of outlet Mach number on optimum pitch to chord ratio (Fig. C)*

$$\Delta g = \frac{g_M - g_{M=0.8}}{g_{M=0.8}} \tag{5.9}$$

Given that we have calculated the chord before, we can now compute the pitch and consequently the number of blades, using the following equation.

$$N_b = \frac{2\pi r^m}{g} \tag{5.10}$$

Obviously, the number of blades must be an integer. As such, the number is rounded to an integer and, using the mean radius, an updated value of g is calculated. The trailing edge thickness is now checked once again, for Fig.6 of [14] (that shall be used in the losses calculation of radial equilibrium theory), which is representative of a large quantity of turbine designs, does not consider values of $\frac{t_e}{g}$ over 0.115, pointing towards the fact that this would lead to very large losses. As such, this value is checked: if the value of $\frac{t_e}{g}$ is smaller or equal to 0.115, the previously calculated number of blades is maintained. However, if the value is larger than 0.115, a new value for t_e is calculated as $t_e = 0.115g$. Again, this value is decreased to 0.5mm, since a larger thickness would only be beneficial if it serves the purpose of cooling. Also, if this is the case now, a warning will be issued alerting for the necessity of a new cooling system. With the new trailing edge thickness calculated, the trailing edge thickness to chord ratio is calculated again and the corrections for the pitch to chord ratio must be computed again, therefore delivering a new pitch. The number of blades is calculated and rounded to an integer. If, throughout the computation, the value of g/c is above 0.9, then the value of 0.9 is assumed, for higher values are not feasible.

Knowing an integer value for the number of blades, we can now compute the value of pitch that will be used in the following mean line analysis computation:

$$g = \frac{2\pi r^m}{N_b} \tag{5.11}$$

5.2.2 Soderberg's Correlation

Soderberg's correlation is a method for obtaining the losses that is based on the space-chord ratio, Reynolds number, aspect ratio (based on axial chord), thickness ratio and blading geometry.

The method is composed of a nominal loss and two corrections, one for the aspect ratio and another for the Reynolds number. The nominal loss is given by the figure 5.6.

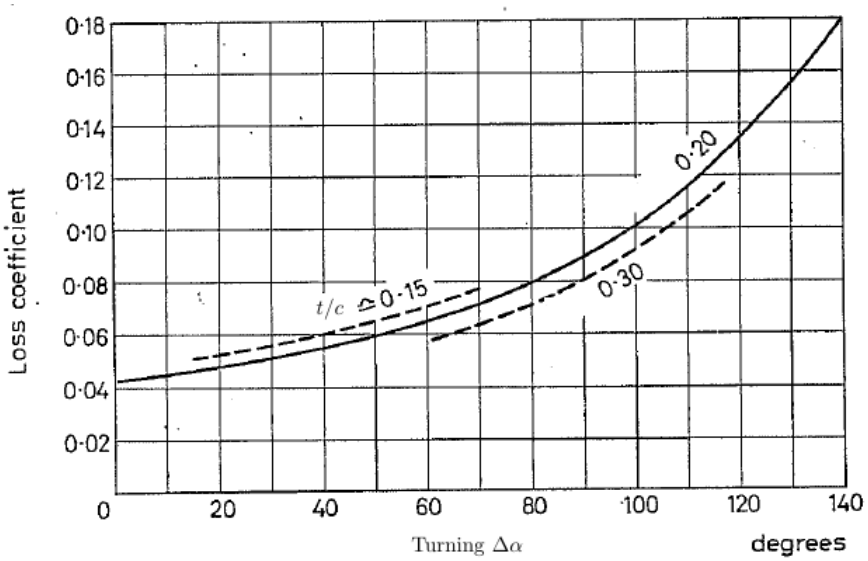

Figure 5.6: *Soderberg's nominal loss coefficient* $\xi^{'}$

The thickness to chord ratio shown as label for the different carpet plots is neglected. At this stage of the design, we simply take the middle curve as reference for this 1D analysis. We notice then, that the nominal loss coefficient will depend only on the turning angle of stator and rotor. The correction for the aspect ratio (based on axial chord) follows.

$$\xi^{''} = \left(1 + \xi^{'}\right)\left(0.975 + 0.075\frac{c_x}{h}\right) - 1 \tag{5.12}$$

[19] suggests that the expression above is valid for rotors, whilst for stators a small correction must be introduced, resulting in the expression below.

$$\xi^{''} = \left(1 + \xi^{'}\right)\left(0.993 + 0.075\frac{c_x}{h}\right) - 1 \tag{5.13}$$

The last correction concerns the Reynolds number.

$$\xi^{'''} = \left(\frac{10^5}{Re_{Dh}}\right)^{1/4} \xi^{''} \tag{5.14}$$

The Reynolds number is based on the hydraulic diameter Dh. According to [9], this is defined as,

$$\text{Stator: } Dh_S = \frac{2hg\cos(\alpha_2)}{g\cos(\alpha_2) + h} \tag{5.15a}$$

$$\text{Rotor: } Dh_R = \frac{2hg\cos(\beta_3)}{g\cos(\beta_3) + h} \tag{5.15b}$$

Hence, the Reynolds number is given by:

$$\text{Stator: } Re_{Dh_S} = \frac{\rho_2 V_2 Dh_S}{\mu_2} \tag{5.16a}$$

$$\text{Rotor: } Re_{Dh_R} = \frac{\rho_3 W_3 Dh_R}{\mu_3} \tag{5.16b}$$

Given this, we can calculate the losses in stator and rotor alike.

5.3 Calculation Procedure

This computation is an iterative process. A value for M_3 is guessed at the beginning of the computation. In the end, a new value for M_3 is found and the cycle restarts until convergence. Several choices and guesses are used along the way (β_3, U, α_2, R_p, η_S, η_R, M_3). In the first approach implemented, the choices made throughout the cycle deliver a turbine with the minimum possible exit Mach number, which translates into a higher efficiency. The implemented cycle is now presented.

By knowing the guessed value of M_3, we are able to find p_3 and T_3:

$$\frac{p_3}{p_{03}} = \left(1 + \frac{\kappa - 1}{2} M_3^2\right)^{\frac{-\kappa}{\kappa - 1}} \tag{5.17}$$

$$\frac{T_3}{T_{03}} = \left(1 + \frac{\kappa - 1}{2} M_3^2\right)^{-1} \tag{5.18}$$

The degree of reaction must now be chosen in order to compute the static pressure T_2. Since the power delivered by the turbine is inversely proportional to the pressure degree of reaction R_p, a minimum value must be used in order to check for feasibility.

$$R_p = \frac{p_2 - p_3}{p_1 - p_3} \tag{5.19}$$

Hence,

$$p_2 = R_p \left(p_1 - p_3\right) + p_3 \tag{5.20}$$

In the first iteration p_1 is unknown. Hence, as a first guess, p_{01} is used instead.

If the rotor process were isentropic then $p_{01} = p_{02}$ and we would have:

$$\frac{p_2}{p_{01}} = \left(1 + \frac{\kappa - 1}{2} M_{2_s}^2\right)^{\frac{-\kappa}{\kappa - 1}} \tag{5.21}$$

Hence, we can apply this to find M_{2_s} and as a consequence T_{2_s}, through (the process is adiabatic, $T_{02} = T_{01}$):

$$\frac{T_{2_s}}{T_{01}} = \left(1 + \frac{\kappa - 1}{2} M_{2_s}^2\right)^{-1} \tag{5.22}$$

We are now able to find V_{2_s}:

$$V_{2_s} = M_{2_s} \sqrt{\kappa R T_{2_s}} \tag{5.23}$$

A new choice arises, now concerning the efficiency of the stator. However, this efficiency can be converged on later by using the results of this computation with Soderberg's correlation.

As such, we can find V_2 with:

$$\eta_S = \frac{V_2^2}{V_{2_s}^2} \tag{5.24}$$

Given that $T_{02} = T_{01}$ (the process is adiabatic) and we know the velocity V_2, we are now able to compute T_2.

$$T_2 = T_{01} - \frac{V_2^2}{2 c_p} \tag{5.25}$$

At this point, two more choices are made. These choices are α_2 and U. Given that M_3 is inversely proportional to both, the highest values possible (given by the user) are used.

Using the turbine velocity triangles theory and conventions presented in the Theoretical Background chapter, we have the following equations:

$$V_2 \cos(\alpha_2) = W_2 \cos(\beta_2) \tag{5.26a}$$

$$V_2 \sin(\alpha_2) = U + W_2 \sin(\beta_2) \tag{5.26b}$$

Since we know V_2, α_2 and U, W_2 and β_2 follow from the two equations above.

The isentropic static temperature at section 3 is calculated using:

$$T_{3_s} = T_2 \left(\frac{p_3}{p_2}\right)^{\frac{k-1}{k}} \tag{5.27}$$

Given that $T_{02}^r = T_{03}^r$ (at mean radius) we have,

$$T_2 + \frac{W_2^2}{2c_p} = T_{3_s} + \frac{W_{3_s}^2}{2c_p} \tag{5.28}$$

Thus enabling the calculation of W_{3_s}.

We can now choose the other efficiency in play, the efficiency of the rotor, with a default value of 0.87. Hence, we can calculate W_3.

$$\eta_R = \frac{W_3^2}{W_{3_s}^2} \tag{5.29}$$

We use a β_3 as high as possible (within user given limits) in order to calculate the tangential velocity in section 3 and then the power available by the turbine. Hence, we have,

$$V_{3_\theta} = W_3 \sin(\beta_3) - U \tag{5.30}$$

We are now able to calculate the power delivered by this turbine:

$$P_{av} = \dot{m} U \left(V_{2_\theta} + V_{3_\theta}\right) \tag{5.31}$$

In order to reach convergence, we must calculate M_3 at the end of this procedure. Using once again the velocity triangles, we may compute V_3 and α_3.

$$V_3 \cos(\alpha_3) = W_3 \cos(\beta_3) \tag{5.32a}$$

$$V_3 \sin(\alpha_3) = U + W_3 \sin(\beta_3) \tag{5.32b}$$

Using the velocity now calculated we can find T_3.

$$T_3 = T_{03} - \frac{V_3^2}{2c_p} \tag{5.33}$$

Finally, we calculate the value of M_3 that will be fed to the beginning of the cycle, until convergence.

$$M_3 = \frac{V_3}{\sqrt{\kappa R T_3}} \tag{5.34}$$

At this point, after the iteration on M_3, we are able to compute the initial conditions, that is, the conditions on the stator inlet.

We first take the mass flow equation for section 1.

$$\dot{m} = \rho_1 A_1 V_{1_x} \tag{5.35}$$

We assume the flow fully axial ($V_{1_x} = V_1$), and the area of section 1 equal to that of section 2. By taking the relation between total temperature, temperature and velocity we can write:

$$V_1 = \sqrt{\left(2c_p T_{01}\left(1 - \frac{T_1}{T_{01}}\right)\right)} = \sqrt{\left(2c_p T_{01}\left(1 - \left(\frac{\rho_1}{\rho_{01}}\right)^{\kappa-1}\right)\right)} \tag{5.36}$$

Since we can calculate ρ_{01} with $\rho_{01} = \frac{p_{01}}{RT_{01}}$, we can discover ρ_1 by iteration. Therefore, V_1 can be calculated.

We now calculate T_1 using:

$$T_1 = T_{01} - \frac{V_1^2}{2c_p} \tag{5.37}$$

And hence we have the desired p_1:

$$p_1 = \rho_1 R T_1 \tag{5.38}$$

We can go back to the calculation with a new initial guess of p_1 to use in equation 5.20. Every time a new value of p_1 is fed back to the beginning of the cycle, the iteration on M_3 must occur again.

At the end of the iteration on p_1, the losses are calculated using Soderberg's correlation, allowing us to find new values to feed back to the beginning of the cycle. Again, every time this happens, until convergence on the losses, new iterations on p_1 must occur, along with the consequent iterations on M_3. We notice that the guesses for M_3 and efficiencies are made in the input file directly. The first guess for p_1 though, is the value for p_{01}, which hence does not come directly from the input file. The convergences present in the MLA are presented in figure 5.7 in a flow chart for better understanding of the iterative processes.

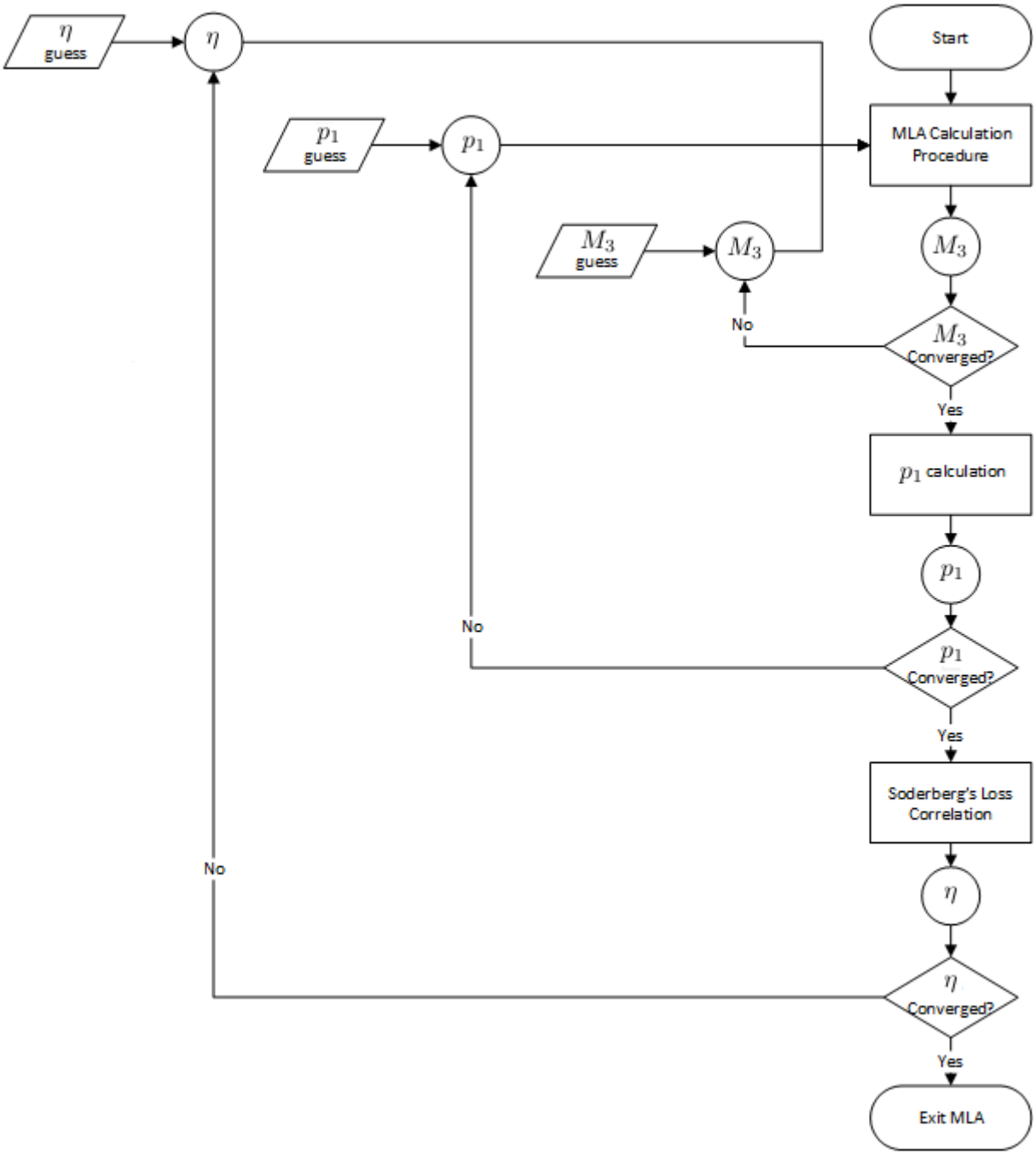

Figure 5.7: *MLA flowchart*

Chapter 6

Design Veracity, Control and Optimization

Several parameters such as efficiency, power and turning angle must be controlled and, in the case of the exit Mach number, optimized, in order to have a reliable and feasible design for the turbine. This section deals with the actions taken to ensure it. All these actions will necessarily demand the rerun of the engine cycle analysis and mean line analysis, until all conditions are met and all iterations have converged.

6.1 Total to Total Efficiency Convergence

It is of great interest to relate the stage total to total efficiency and the losses in the stator and rotor. We can first rewrite equation 3.35 as:

$$\eta_{TT} = \frac{h_{01} - h_{03}}{(h_{01} - h_{03}) + (h_{03} - h_{03_{ss}})} \tag{6.1}$$

Taking into account figure 3.2 and assuming that we have a negligible divergence between the p_2 and p_3 isobars, we can assume that the total enthalpy loss is equal to the sum of the enthalpy losses in stator and rotor.

$$(h_{03} - h_{03_{ss}}) = (h_3 - h_{3_s}) + (h_2 - h_{2_s}) \tag{6.2}$$

Also, we can rewrite equation 3.44 as, for stator and rotor, respectively:

$$\xi_S = \frac{h_2 - h_{2_s}}{\frac{V_2^2}{2}} \tag{6.3a}$$

$$\xi_R = \frac{h_3 - h_{3_s}}{\frac{W_3^2}{2}} \tag{6.3b}$$

Finally, rearranging equations 6.3, applying them on equation 6.2 and substituting on 6.1, we get the result we were looking for.

$$\eta_{TT} = \frac{1}{1 + \frac{\xi_S \frac{V_2^2}{2} + \xi_R \frac{W_3^2}{2}}{h_{01} - h_{03}}} \tag{6.4}$$

Therefore, at the end of the mean line analysis, we have a new value for the parameter η_{TT} that was given as a guess to the engine cycle analysis. Thus, we are able to iterate between the engine cycle analysis and the mean line analysis (η_{gg}) in order to find a consistent solution for the turbine in terms of efficiency.

6.2 Exit Mach Number Optimization

The exit Mach number M_3 should be as low as possible. The initial guesses made in the mean line analysis are such that they allow for the smallest possible exit Mach number. It is observable that the general trends in the variables that allow for a smallest as possible exit Mach number are, within user given limits:

- R_p as low as possible;
- α_2 as high as possible;
- U as high as possible;
- β_3 as high as possible;

These are only general individual trends of these variables. It is not ensured that a different combination of these variables would eventually allow for a slightly smaller M_3. However, in the scope of a preliminary design, this is a fast and considerably good way of reaching a good turbine design. We now take into attention the case of the mean rotation velocity U. Its increase allows not only a decrease in M_3, but also an immediate increase in power (equation 6.5b). However, this value is typically limited to a maximum of 500 m/s at the tip due to material limitations. Hence, the initial guess for U is changed, using the values for the radius calculated at each iteration, until the program arrives at a $U^t \approx 500$ m/s. Thus, all designs resultant from this program will have a fixed U^t of about 500 m/s. The other variables, R_p, α_2 and β_3 are subject to change only if really necessary for the purpose of power or design control.

6.3 Power Availability

The power delivered by the turbine was calculated in different ways in the engine cycle analysis and the mean line analysis. These are, respectively:

$$P_{ECA} = \dot{m} c_p \left(T_{01} - T_{03}\right) \tag{6.5a}$$

$$P_{MLA} = U \left(V_{2_\theta} + V_{3_\theta}\right) \tag{6.5b}$$

Given that the total to total efficiency is being iterated on until convergence, it is expected that the power delivered is the same independently of the formula. Since the convergence is never perfect however, small changes may arise. Also, the values imposed to design variables such as α_2, β_3 and R_p may not be able to deliver a turbine with the desired power. Therefore, change must be operated in these variables in order to ensure that the power delivered by the turbine designed in the mean line analysis is equal or larger to the one demanded by the engine cycle analysis.

Hence, in the case that $P_{MLA} < P_{ECA}$ the following action is taken, in order of desirability, according to whatever can help in minimizing M_3 or at least harm this minimization the least (second and third choices are only activated if the previous choice is no longer possible due to imposed variable limits).

1. Increase α_2;
2. Decrease R_p;
3. Increase β_3;

In the extreme case that no more change is available, the program finishes with a warning for the user, since the initial data given to the program does not allow for a feasible design.

6.4 Design Control

In the design control, as in the power availability, the changes that may be necessary occur in a certain order of preference of variable, according to whatever can help in minimizing M_3 or at least harm this minimization the least. This control is mostly based on guide lines given in [10], along with suggested actions.

1. The first control point concerns the value of M_2. This value should be between 0.85 and 1.2. According to [10], high subsonic values are typical of a high enthalpy reaction, whereas the low supersonic can be linked to a medium enthalpy reaction. Actions:
   (a) Increase R_p if $M_2 > 1.2$;
   (b) Decrease R_p if $M_2 < 0.85$;
2. The next check point concerns the angle β_2 and M_2^r. β_2 should not be larger than 45° and M_2^r should be inferior to 0.5. The action taken to achieve both inequalities is the same, since they are intricately connected. Actions:
   (a) Decrease α_2;
   (b) Increase R_p;
3. The turning angle of the rotor $\beta_2 + \beta_3$ must be inferior to 110°. Higher values are possible, but one must impose a smaller limit for the mean line analysis since the turning may increase from the mean radius to one of the walls (which can happen when the 2D analysis takes place). Actions:
   (a) Decrease α_2;
   (b) Increase R_p;
   (c) Decrease β_3;
4. The relative rotor exit Mach number, M_3^r, should belong in the same interval as M_2 or slightly higher. However, contrary to what happened with M_2, a low supersonic Mach number corresponds to a high enthalpy reaction and a high subsonic value to a medium enthalpy reaction. Actions:

(a) Increase R_p if $M_3^r < 0.85$;

(b) Decrease R_p if $M_3^r > 1.3$;

(c) Decrease β_3 if $M_3^r < 0.85$;

(d) Increase β_3 if $M_3^r > 1.3$;

5. The height ratio between rotor exit and stator exit must also be controlled, in order to avoid losses due to flow separation in the oblique walls that must exist to allow for a rotor exit height higher than the stator exit height. The maximum value for this ratio has been fixed in 1.2. Actions:

   (a) Increase α_2;

   (b) Decrease β_3;

6. Finally, α_3 must be kept below 30°. Actions:

   (a) Decrease β_3;

It may happen that two requirements may demand counter-actions, that is, for example, one requirement demands an increase in R, and another demands a decrease in R. If so, when finding a counter-action, the program does not change this variable and moves on to the second option, hence trying to meet the second requirement using another variable. If this is successful, the program can now work with the first variable in order to meet the first requirement.

Chapter 7

Radial Equilibrium

The theory presented in section 3.6 will be applied first assuming isentropic behaviour (ISRE - Isentropic Simple Radial Equilibrium) and later taking into account losses (Non-Isentropic Simple Radium Equilibrium), in order to include entropy effects. The tangential velocity distributions used in RET will be presented in the following section. Next, the calculation procedure for the ISRE will be presented, followed by the loss calculation according to [14] and finally the calculation procedure for the NISRE.

7.1 ISRE

We start by taking the radium equilibrium equation:

$$\frac{dh_0}{dr} - T\frac{ds}{dr} = \frac{V_\theta}{r}\frac{d\left(rV_\theta\right)}{dr} + V_x\frac{dV_x}{dr} \tag{7.1}$$

We know that $\frac{dh_0}{dr} = 0$ and, since we are assuming isentropic behaviour, $\frac{ds}{dr} = 0$.

Hence, the resultant equation is:

$$V_x\frac{d\left(V_x\right)}{dr} = -\frac{V_\theta}{r}\frac{d\left(rV_\theta\right)}{dr} \tag{7.2}$$

Therefore, by admitting a certain tangential velocity distribution, we can compute the axial velocity. Several classical tangential velocity distributions are used. These distributions are special cases of a more general distribution:

$$V_\theta = Ar^n \pm \frac{B}{r} \tag{7.3}$$

The plus sign corresponds to the flow downstream of the rotor and the minus sign corresponds to the flow upstream of the rotor. The three different cases programmed correspond to A=0, which is called the Free Vortex design, n=1, the so-called Constant Degree of Reaction design, and n=0, also known as Exponential design. An important note regarding the equation above is that it is written considering the direction of the axis as positive in the direction of rotation when downstream of the rotor. This goes against the convention used in this document. However, for the sake of uniformity with most documents regarding this subject, the expressions are kept for this part of the calculation only. In the end, the results are translated to the convention used in the document, so that they can be used for other sections of the design exercise.

Vortex Design

In Free Vortex Design we have:

$$V_\theta = \frac{B}{r} \tag{7.4}$$

We can determine B (different for the stator and for the rotor) using $V_\theta^m = \frac{B}{r^m}$. Then, substituting the tangential velocity distribution in 7.2, we obtain:

$$V_x \frac{d\left(V_x\right)}{dr} = 0 \tag{7.5}$$

Therefore, we arrive at the very important result that, in Free Vortex design,

$$V_x = const. \tag{7.6}$$

Finding this constant axial velocity is the main purpose of the calculation.

Constant Degree of Reaction Design

In this design we have:

$$V_\theta = Ar \pm \frac{B}{r} \tag{7.7}$$

Since we know that A and B must be the same in front and behind the rotor, we can use mean line analysis data to write:

$$V_{2_\theta}^m = Ar_2^m - \frac{B}{r_2^m} \tag{7.8a}$$

$$V_{3_\theta}^m = Ar_3^m + \frac{B}{r_3^m} \tag{7.8b}$$

We now have two equations with two unknowns, which we can extract easily. Substituting the expression for V_θ in 7.2 we have, behind the stator:

$$V_x \frac{d\left(V_x\right)}{dr} = -\frac{V_\theta}{r} \frac{d\left(rV_\theta\right)}{dr} \tag{7.9}$$

$$V_x \frac{d\left(V_x\right)}{dr} = -\frac{V_\theta}{r} \frac{d\left(Ar^2\right)}{dr} \tag{7.10}$$

$$V_x \frac{d\left(V_x\right)}{dr} = -\frac{V_\theta}{r} 2Ar \tag{7.11}$$

$$V_x \frac{d\left(V_x\right)}{dr} = \left(-A + \frac{B}{r^2}\right) 2Ar \tag{7.12}$$

Integrating this from the mean radius to any radius of our choice we have:

$$\int_{V_{2_x}^m}^{V_{2_x}} V_x dV_x = \int_{r_2^m}^{r_2} -2A^2 r + \frac{2AB}{r} dr \tag{7.13}$$

Hence, we have,

$$V_{2_x} = \sqrt{-2A^2\left(r_2^2 - r_2^{m\,2}\right) + 4AB \ln\left(\frac{r_2}{r_2^m}\right) + V_{2_x}^{m\,2}} \tag{7.14}$$

The same can be derived for the flow behind the rotor, with the following result:

$$V_{3_x} = \sqrt{-2A^2\left(r_3^2 - r_3^{m\,2}\right) - 4AB \ln\left(\frac{r_3}{r_3^m}\right) + V_{3_x}^{m\,2}} \tag{7.15}$$

In this case, finding $V_{2_x}^m$ and $V_{3_x}^m$ will be the key to solve the radial equilibrium analysis.

Exponential Design

The determination of the mathematical expressions used for this design is in everything similar to the constant degree of reaction design. We have the following tangential velocity distribution:

$$V_\theta = A \pm \frac{B}{r} \tag{7.16}$$

Since we know that A and B must be the same in front and behind the rotor, we can use mean line analysis data to write:

$$V_{2_\theta}^m = A - \frac{B}{r_2^m} \tag{7.17a}$$

$$V_{3_\theta}^m = A + \frac{B}{r_3^m} \tag{7.17b}$$

Once again, we have two equations with two unknowns, therefore enabling the calculation of A and B. Substituting the expression for V_θ in 7.2 we have, behind the stator:

$$V_x \frac{d\left(V_x\right)}{dr} = -\frac{V_\theta}{r} \frac{d\left(rV_\theta\right)}{dr} \tag{7.18}$$

$$V_x \frac{d\left(V_x\right)}{dr} = -\frac{V_\theta}{r} \frac{d\left(Ar\right)}{dr} \tag{7.19}$$

$$V_x \frac{d\left(V_x\right)}{dr} = -\frac{V_\theta}{r} A \tag{7.20}$$

$$V_x \frac{d\left(V_x\right)}{dr} = \left(-\frac{A}{r} + \frac{B}{r^2}\right) A \tag{7.21}$$

Integrating this from the mean radius to any radius of our choice we have:

$$\int_{V_{2_x}^m}^{V_{2_x}} V_x dV_x = \int_{r_2^m}^{r_2} -\frac{A^2}{r} + \frac{AB}{r^2} dr \tag{7.22}$$

Hence, we have,

$$V_{2_x} = \sqrt{-2A^2 \ln\left(\frac{r_2}{r_2^m}\right) - 2AB\left(\frac{1}{r_2} - \frac{1}{r_2^m}\right) + {V_{2_x}^m}^2} \tag{7.23}$$

The same can be derived for the flow behind the rotor, with the following result:

$$V_{3_x} = \sqrt{-2A^2 \ln\left(\frac{r_3}{r_3^m}\right) + 2AB\left(\frac{1}{r_3} - \frac{1}{r_3^m}\right) + {V_{3_x}^m}^2} \tag{7.24}$$

Once again, finding $V_{2_x}^m$ and $V_{3_x}^m$ will be the key to solve the radial equilibrium analysis.

7.1.1 Calculation Procedure

The iterative process applied for the ISRE will now be presented. A first initial guess of V_x^m is taken as larger than the value from the mean line analysis. The value is taken larger than the one from mean line analysis in order to avoid calculations that may deliver imaginary numbers, such as the square root of a negative number, as might happen in the exponential design equation for axial speed. As such, using the constants previously computed and this initial guess, we can compute the entire velocity distribution for any given radius.

The iterative cycle is composed of 4 main equations, all dependent on the radius through the expressions of the tangential and axial velocity. These 4 equations are now presented.

$$T_2(r_2) = T_{01} - \frac{1}{2c_p}\left(V_{2_x}^2(r_2) + V_{2_\theta}^2(r_2)\right) \tag{7.25a}$$

$$p_2(r_2) = p_{01}\left(\frac{T_2(r_2)}{T_{01}}\right)^{\frac{\kappa}{\kappa-1}} \tag{7.25b}$$

$$\rho_2(r_2) = \frac{p_2(r_2)}{RT_2(r_2)} \tag{7.25c}$$

$$\dot{m} = \int_{r_2^h}^{r_2^t} 2\pi r_2 \rho_2(r_2) V_{2_x}(r_2) dr \tag{7.25d}$$

We remark the important detail of equation 7.25b using p_{01} ($p_{02}^r(r_3)$ in equation 7.26c), representing the non-existence of losses in this computation, and the use of T_{01} in equation 7.25a ($T_{03}^r(r_3)$ in equation 7.26b), which translates as adiabatic flow. After performing this calculation for the stator, we are able to calculate p_{02}^r, equation 7.41b, and T_{02}^r, equation 7.38c, which will be used for the same type of computation for the rotor, as described below. In fact, relative quantities are used for the rotor calculation, forcing the appearance of one more equation to calculate W_{3_θ}.

$$W_{3_\theta}(r_3) = V_{3_\theta}(r_3) + \Omega r_3 \tag{7.26a}$$

$$T_3(r_3) = T_{03}^r(r_3) - \frac{1}{2c_p}\left(W_{3_x}^2(r_3) + W_{3_\theta}^2(r_3)\right) \tag{7.26b}$$

$$p_3(r_3) = p_{02}^r(r_3)\left(\frac{T_3(r_3)}{T_{03}^r(r_3)}\right)^{\frac{\kappa}{\kappa-1}} \tag{7.26c}$$

$$\rho_3(r_3) = \frac{p_3(r_3)}{RT_3(r_3)} \tag{7.26d}$$

$$\dot{m} = \int_{r_3^h}^{r_3^t} 2\pi r_3 \rho_3(r_3) V_{3_x}(r_3) dr \tag{7.26e}$$

These integrations are performed using the trapezoidal rule, given by equation 3.54. These integrals were performed in 20 sections along the radius. For each section, the equations above were computed for the beginning and finishing radius of that section, in order to use the trapezoidal rule.

In the end, the value obtained for $\dot{m}$ is compared to the one calculated in the engine cycle analysis. The initial guess of V_x^m is changed accordingly, until convergence, which means, for example, that if the mass flow value calculated is smaller than the one from ECA, the mean axial velocity is increased accordingly to a higher value. The criteria for the change performed in V_x^m according to the difference between mass flows are summed up in the following table.

$m_{calc.} - m_{ECA}$	V_x^m
]-∞ ; -1[	V_x^m+10
[-1 ; -0.1[	V_x^m+0.1
[-0.1 ; -0.01[	V_x^m+0.01
[-0.01 ; -0.001[	V_x^m+0.001
[-0.001 ; -0[	V_x^m+0.0001
[0 ; -0.001[	V_x^m−0.0001
[-0.001 ; -0.01[	V_x^m−0.001
[-0.01 ; -0.1[	V_x^m−0.01
[-0.1 ; 1[	V_x^m−0.1
[1 ; ∞[	V_x^m−10

Table 7.1: *Criteria to achieve convergence between $m_{calc.}$ and m_{ECA}*

7.1.2 Results Display

After the calculation procedure presented before, the results from this computation are presented at 21 different lines, that is, at lines separated by a length equal to 5% of the difference between tip and hub radii (the same lines that limit the different sections in which the previous integral was calculated). All the data presented have their sole origin on the velocity distributions from the radial equilibrium and on total conditions data.

We first compute the initial conditions (stator inlet), as done at the mean line analysis with the purpose of finding p_1, but with the updated values from the ISRE computation.

Also, we must now take into account U as variable with the radius, as it was done in equation 7.26a, since we have a changing radius and therefore can only take the rotation speed Ω as constant.

To calculate Ω, the mean radius at section 2 is taken as reference, along with the mean line analysis rotation speed U^m.

$$\Omega = \frac{U^m}{r_2^m} \tag{7.27}$$

At this point, it is possible to calculate all the values necessary for the forthcoming design stages. For each parallel line (represented by i, varying from 0 to 20), the following figures are calculated:

$$r(\%) = 0.05 \times i \times 100 \tag{7.28}$$

$$r_2 = r_2^h + \frac{r(\%) \times \left(r_2^t - r_2^h\right)}{100} \tag{7.29a}$$

$$r_3 = r_3^h + \frac{r(\%) \times \left(r_3^t - r_3^h\right)}{100} \tag{7.29b}$$

$$U_2 = \Omega r_2 \tag{7.30a}$$

$$U_3 = \Omega r_3 \tag{7.30b}$$

$$\text{Free Vortex Design: } V_{2_x} = V_{2_x}^m \tag{7.31a}$$

$$\text{Constant DR Design: } V_{2_x} = \sqrt{-2A^2\left(r_2^2 - r_2^{m\,2}\right) + 4AB\ln\left(\frac{r_2}{r_2^m}\right) + V_{2_x}^{m\,2}} \tag{7.31b}$$

$$\text{Exponential Design: } V_{2_x} = \sqrt{-2A^2\ln\left(\frac{r_2}{r_2^m}\right) - 2AB\left(\frac{1}{r_2} - \frac{1}{r_2^m}\right) + V_{2_x}^{m\,2}} \tag{7.31c}$$

$$\text{Free Vortex Design: } V_{3_{ax}} = V_{3_x}^m \tag{7.32a}$$

$$\text{Constant DR Design: } V_{3_{ax}} = \sqrt{-2A^2\left(r_3^2 - r_{3m}^2\right) - 4AB\ln\left(\frac{r_3}{r_{3m}}\right) + V_{3_x}^{m\,2}} \tag{7.32b}$$

$$\text{Exponential Design: } V_{3_x} = \sqrt{-2A^2\ln\left(\frac{r_3}{r_3^m}\right) + 2AB\left(\frac{1}{r_3} - \frac{1}{r_3^m}\right) + V_{3_x}^{m\,2}} \tag{7.32c}$$

$$\text{Free Vortex Design: } V_{2_\theta} = \frac{B}{r_2} \tag{7.33a}$$

$$\text{Constant DR Design: } V_{2_\theta} = Ar_2 - \frac{B}{r_2} \tag{7.33b}$$

$$\text{Exponential Design: } V_{2_\theta} = A - \frac{B}{r_2} \tag{7.33c}$$

$$\text{Free Vortex Design: } V_{3_\theta} = \frac{B}{r_3} \tag{7.34a}$$

$$\text{Constant DR Design: } V_{3_\theta} = Ar_3 + \frac{B}{r_3} \tag{7.34b}$$

$$\text{Exponential Design: } V_{3_\theta} = A + \frac{B}{r_3} \tag{7.34c}$$

$$V_2 = \sqrt{V_{2_x}^2 + V_{2_\theta}^2} \tag{7.35a}$$

$$V_3 = \sqrt{V_{3_x}^2 + V_{3_\theta}^2} \tag{7.35b}$$

$$W_2 = \sqrt{V_{2_x}^2 + \left(V_{2_\theta} - U_2\right)^2} \tag{7.35c}$$

$$W_3 = \sqrt{V_{3_x}^2 + \left(V_{3_\theta} + U_3\right)^2} \tag{7.35d}$$

$$\alpha_2 = \arctan\left(\frac{V_{2_\theta}}{V_{2_x}}\right) \tag{7.36a}$$

$$\alpha_3 = \arctan\left(\frac{V_{3_\theta}}{V_{3_x}}\right) \tag{7.36b}$$

$$\beta_2 = \arctan\left(\frac{V_{2_\theta} - U_2}{V_{2_x}}\right) \tag{7.36c}$$

$$\beta_3 = \arctan\left(\frac{V_{3_\theta} - U_3}{V_{3_x}}\right) \tag{7.36d}$$

$$\Delta\alpha_S = \alpha_1 + \alpha_2 \tag{7.37a}$$

$$\Delta\alpha_R = \beta_2 + \beta_3 \tag{7.37b}$$

$$T_1 = T_{01} - \frac{V_1^2}{2c_p} \tag{7.38a}$$

$$T_2 = T_{01} - \frac{V_2^2}{2c_p} \tag{7.38b}$$

$$T_{03}^r = T_{02}^r - \frac{U_2^2}{2c_p} + \frac{U_3^2}{2c_p} = T_2 + \frac{W_2^2}{2c_p} - \frac{U_2^2}{2c_p} + \frac{U_3^2}{2c_p} \tag{7.38c}$$

$$T_3 = T_{03}^r - \frac{W_3^2}{2c_p} \tag{7.38d}$$

$$M_2 = \frac{V_2}{\kappa R T_2} \tag{7.39a}$$

$$M_3 = \frac{V_3}{\kappa R T_3} \tag{7.39b}$$

$$M_2^r = \frac{W_2}{\kappa R T_2} \tag{7.39c}$$

$$M_3^r = \frac{W_3}{\kappa R T_3} \tag{7.39d}$$

$$R_h = \frac{T_2 - T_3}{T_1 - T_3} \tag{7.40}$$

$$p_2 = p_{01} \left(\frac{T_2}{T_{01}} \right)^{\frac{\kappa}{\kappa - 1}} \tag{7.41a}$$

$$p_{03}^r = p_{02}^r = p_2 \left(1 + \frac{\kappa - 1}{2} (M_2^r)^2 \right)^{\frac{\kappa}{\kappa - 1}} \tag{7.41b}$$

$$p_3 = p_{02}^r \left(1 + \frac{\kappa - 1}{2} (M_3^r)^2 \right)^{\frac{-\kappa}{\kappa - 1}} \tag{7.41c}$$

7.2 Losses

This loss section is mainly based on reference [14]. The losses can be divided into the following types: profile losses, secondary losses, annulus losses and leakage losses. [14] presents a step-by-step calculation procedure for the calculation of these losses through several coefficients. It is important to notice though, that these coefficients, as calculated in [14], are in percentage. Also, they must be summed, according to whichever distribution they have (for example the leakage losses will only occur at the tip). X, the total loss calculated from [14] corresponds to the loss in kinetic energy referred to the real velocity, as presented in equation 3.44.

7.2.1 Previous Considerations

Some aspects of the turbine geometry must be computed before starting the losses calculation. Also, angles convention is discussed.

Angles

The angles definition used in [14] is different from the one used in this document. In fact, the angles used in the paper can be calculated from the original angles in this document according to table 7.2. For simplicity, in this section, whenever any angle is referred to, it corresponds to the definition in [14] (German convention).

$angles_{[\mathbf{14}]}$	$angles_{doc.}$
$\alpha_{2[14]}$	$90 - \alpha_{2doc.}$
$\beta_{2[14]}$	$90 - \beta_{2doc.}$
$\alpha_{3[14]}$	$90 - \alpha_{3doc.}$
$\beta_{3[14]}$	$90 - \beta_{3doc.}$

Table 7.2: *Conversion between $angles_{[14]}$ and the $angles_{doc.}$*

Other geometric properties

Section 5.2.1 is here recovered, for it is of utmost importance for what is to follow. At this point, all the geometric calculations in that section are updated with mean radius values from the ISRE, especially since the number of blades is an obvious figure to take as calculation constant throughout the radius. As such, the mean radius position is used and considered representative of the turbine for the computation of these geometric properties: chord, trailing edge thickness and number of blades.

7.2.2 Profile Losses

The profile losses are the losses related to the friction on the blade profiles and also to the blade wakes. For the profile loss calculation, the incidence angles are supposed to be zero (which is desired as this is a design exercise and an optimized design would have $i = 0$). Also, the blades are assumed to be straight backed blades, since a back surface radius different from zero would mean higher profile losses. For each radial position, the following quantities, necessary for the calculation of the profile losses, are computed. When necessary, distinction between equations for the stator and the rotor is provided.

$$g = \frac{2\pi r}{N_b} \tag{7.42}$$

$$\frac{g}{b} = \frac{\frac{g}{c}}{0.72 + 0.005\Delta\alpha} \tag{7.43}$$

Equation 7.43 is taken from [10].

$$\text{Stator: } o = g\sin(\alpha_2) \tag{7.44a}$$

$$\text{Rotor: } o = g\sin(\beta_3) \tag{7.44b}$$

This is the so-called sine-rule for the outlet angle. As it can be observed in figure 7.1, the angles referred are measured from the meridional axis, that is, the same convention as used in [14].

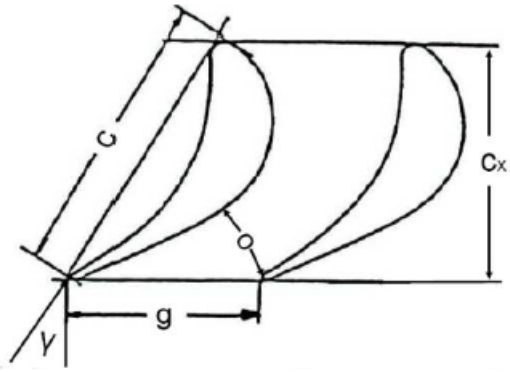

Figure 7.1: *Sine-rule geometry for the outlet angle*

Sutherland's Law was used in order to calculate the dynamic viscosity and therefore we are able to calculate the density for each radial position and for both stator and rotor.

$$\rho = \frac{p}{RT} \tag{7.45}$$

Finally, the Reynolds number with respect to the throat size is calculated with:

$$\text{Stator: } Re_o = \frac{\rho V_2 o}{\mu} \tag{7.46a}$$

$$\text{Rotor: } Re_o = \frac{\rho W_3 o}{\mu} \tag{7.46b}$$

We are now able to use the plots from [14] in order to calculate the profile losses. The profile loss factor in the correlation proposed in [14] is given by the following equation.

$$X_p = x_{pb} N_{pr} N_{pt} N_{pi} + (\Delta x_p)_t + (\Delta x_p)_{s/e} + (\Delta x_p)_m \tag{7.47}$$

N_{pr} presents the effect of the Reynolds number on the profile loss ratio, x_{pb} is the basic profile loss parameter, N_{pt} gives a correction on the profile loss ratio based on the trailing edge thickness over pitch ratio, N_{pi} is a correction on the profile loss ratio due to incidence losses. $(\Delta x_p)_t$ is a further increment on the profile losses based on the trailing edge thickness over pitch ratio, $(\Delta x_p)_{s/e}$ is another correction to account for blade back radius losses and finally $(\Delta x_p)_m$ is yet another increment, to account for Mach number effects.

As referred before, incidence angles are assumed to be zero. As such, according to Fig.10 of [14], $N_{pi} = 1$. Since all blades are considered to be straight backed blades, $(\Delta x_p)_{s/e} = 0$. As such, we have,

$$X_p = x_{pb} N_{pr} N_{pt} + (\Delta x_p)_t + (\Delta x_p)_m \tag{7.48}$$

N_{pr} is based on a plot that depends on the smoothness of the blades. A standard finish is assumed, which corresponds to the value of 0.1, as we can observe in figure 7.2.

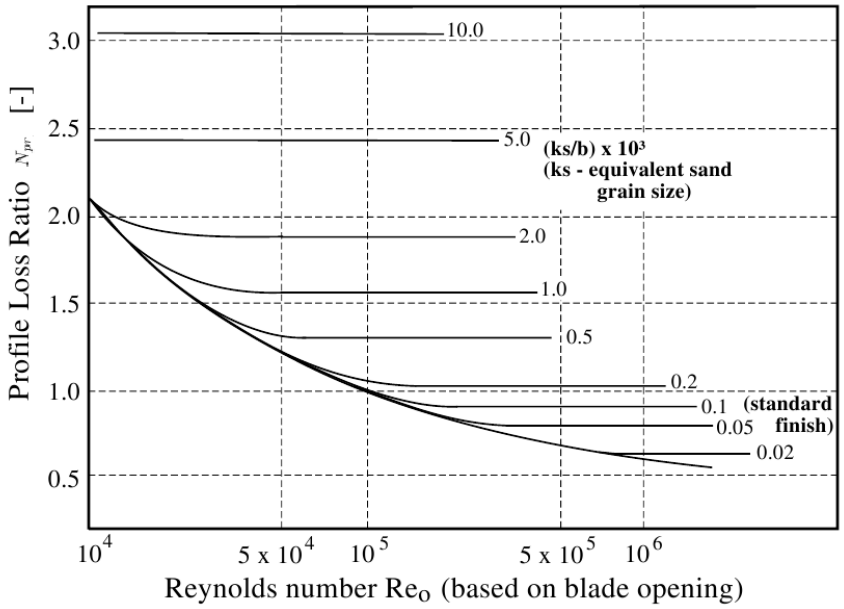

Figure 7.2: *Profile loss ratio against Reynolds number effect [14][15]*

As such, by using the value of Re_o calculated before, we are able to compute N_{pr}.

If we look at the plot for x_{pb} (figure 7.3), we observe that we must first know the contraction ratio (figure 7.5) and the modified lift coefficient (figure 7.4), given by $F_L\,(g/b)$.

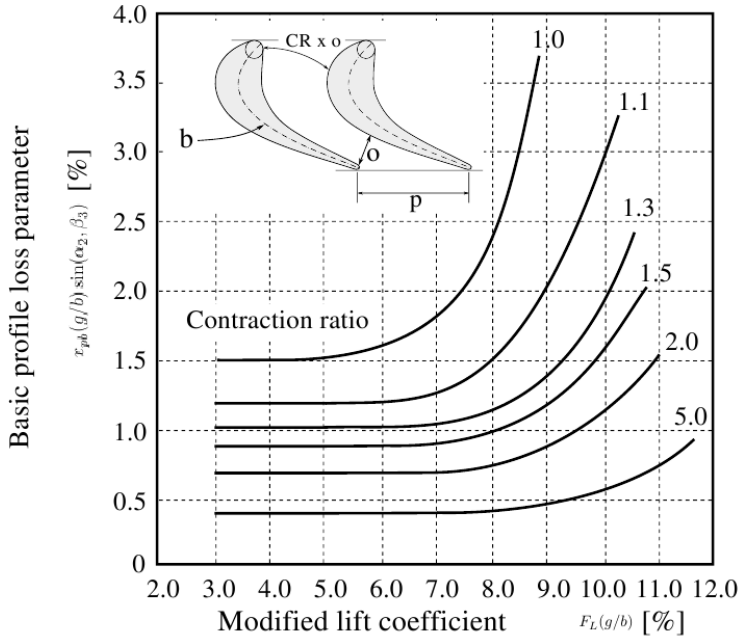

Figure 7.3: *Basic profile loss [14][15]*

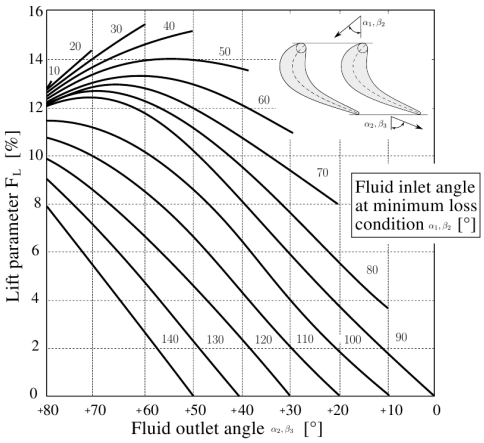

Figure 7.4: *Lift parameter, F_L [14][15]*

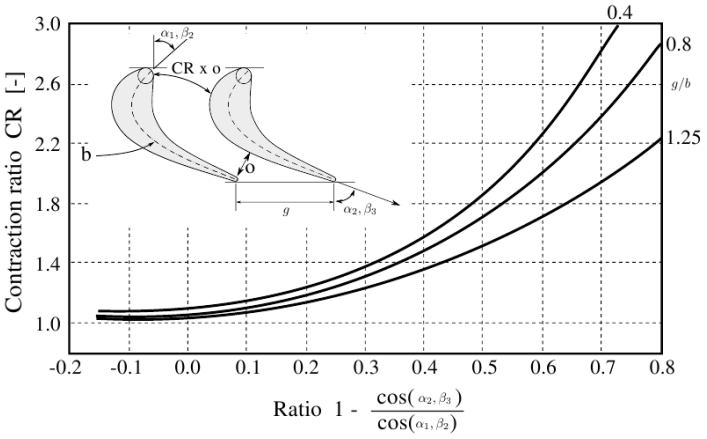

Figure 7.5: *Contraction ratio for average profiles [14][15]*

In order to calculate F_L, we need but the inlet and outlet angles, remembering the convention of [14], whilst for the contraction ratio C.R. we also need the pitch to backbone length ratio that was calculated previously. After calculating these two figures, we are now able to calculate x_{pb}.

The carpet plot for calculating N_{pt} and $(\Delta x_p)_t$ is presented in figure 7.6.

In fact, for N_{pt} we need the fluid outlet angle and t_e/g, both of which we already have. For $(\Delta x_p)_t$ we just need t_e/g.

Figure 7.7, taken from [14], gives the correlation for $(\Delta x_p)_m$, which is based on arcsin $\left(\frac{o+t_e}{g}\right)$ and on the relative outlet isentropic Mach number. We have the latter and the first is easily calculated.

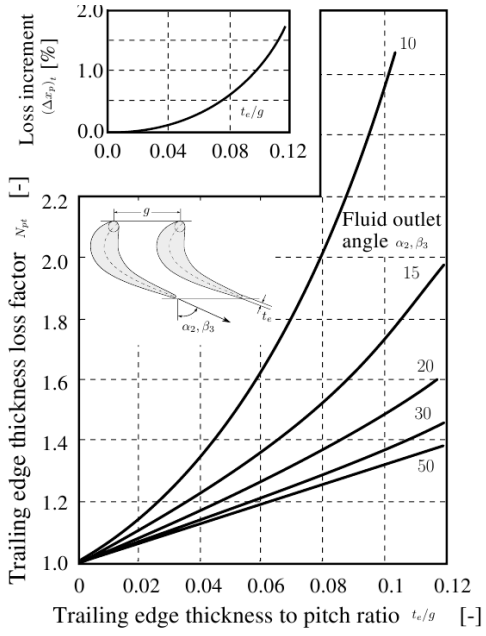

Figure 7.6: *Trailing edge thickness losses [14][15]*

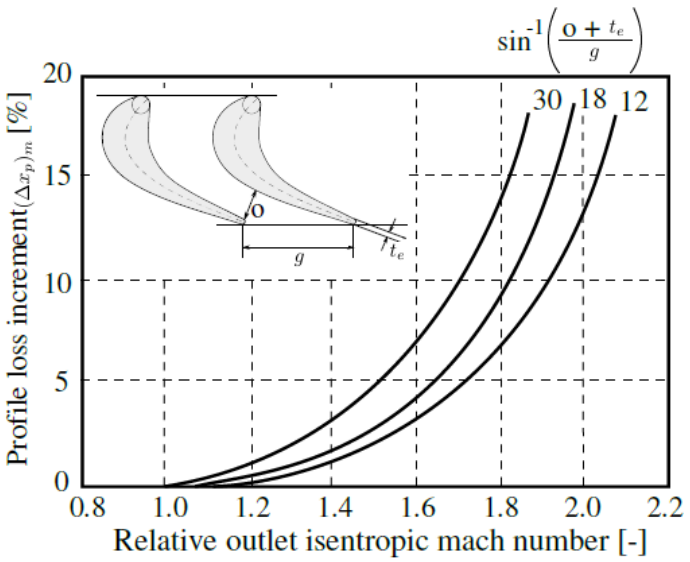

Figure 7.7: *Mach number loss for convergent blading [14][15]*

We can now calculate the profile loss factor.

7.2.3 Secondary Losses

The secondary losses are the losses related to the friction on the walls at root and tip, together with any other end effects. Given this, it is obvious that secondary losses occur mainly at the hub and tip and seldomly at mean radius. Instead of calculating the losses for several lines parallel to the walls, we actually get only two values from [14], using hub and tip radii values. Each of these values represents an overall integrated value of the secondary losses. The reason for the calculation of two values, one at hub and another at tip, instead of only one at the mean radius, lies with the possible asymmetry in the secondary losses distribution. Having two values, we are able to ponder on the amount of secondary losses distribution for either hub or tip. After calculated, the secondary losses must be redistributed. First, however, the process for finding a value for the secondary losses from [14] will be explained. All the calculations here presented are performed the same way for stator and rotor.

According to [14], the secondary losses are given by:

$$X_s = (N_s)_r \, (N_s)_{h/b} \, (x_s)_b \tag{7.49}$$

$(N_s)_r$ is the same Reynolds number correction used for the profile losses, $(N_p)_r$. This corresponds to figure 7.2. The plots for $(N_s)_{h/b}$ (secondary loss ratio against aspect ratio factor) and $(x_s)_b$ (basic secondary loss parameter) are presented below in figures 7.8 and 7.9, respectively.

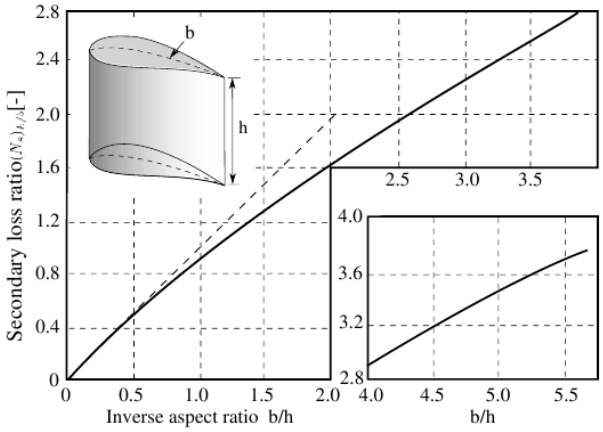

Figure 7.8: *Secondary loss-aspect ratio factor [14][15]*

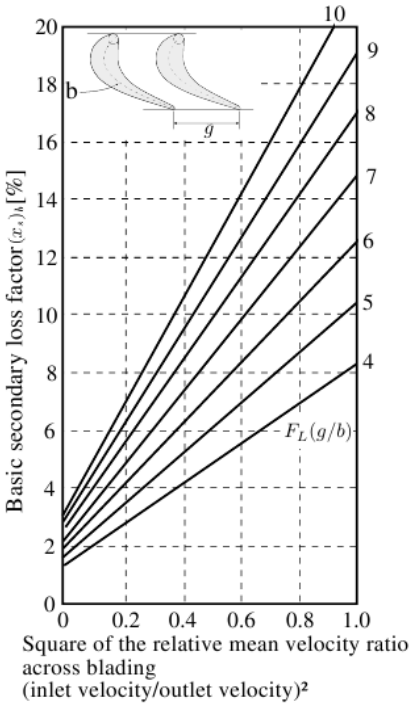

Figure 7.9: *Secondary loss-basic loss factor [14][15]*

All the quantities necessary for these plots have been previously calculated: backbone length, blade height, lift parameter, pitch, chord and inlet and outlet velocities for both stator and rotor. Again, all the values used correspond to the hub and tip radii.

We can now proceed to the redistribution of these losses. Two decisions must be made concerning this redistribution. The first is the level of penetration of the secondary losses. This is the percentage of blade

height, starting from the walls, that is affected by the secondary loss of each wall. The second decision is the type of distribution of these losses. The secondary losses are higher at the walls and decrease to zero when reaching the point on the radius previously defined with the level of penetration. This variation may be modelled in two ways: with a linear distribution or a parabolic distribution. The integral of these curves inside the radius defined by the level of penetration must be equal to the integral of the average of the values found in [14] using the hub and tip radii values.

As suggested in [17], an averaged value for the secondary losses can be found with a sort of mass averaging of the secondary losses at the hub and tip, through the following expression.

$$\zeta_s = \frac{\left(\frac{V^h}{V^m}\right)^2 \zeta_s^h + \frac{r^t}{r^h}\left(\frac{V^t}{V^m}\right)^2 \zeta_s^t}{1 + \frac{r^t}{r^h}} \tag{7.50}$$

However, in [14] the losses are defined as described in equation 3.44. Hence, in order to use equation 7.50, the coefficients must be transformed using equation 3.45c. In the end, the value is converted back and hence we find the final value for the secondary losses from the Craig & Cox correlation, $(X_s)_{CC}$.

Level of Penetration

[14] does not present any indication concerning this topic. However, Holliger [18], defines a critical aspect ratio (based on pitch), depending on the profile losses, at which the secondary flow regions extend to half the blade height. This correlation, adapted by [10], is given by:

$$\left(\frac{h}{g}\right)_{cr} = 7 \rightarrow 10\sqrt{\zeta_p} \tag{7.51}$$

Four critical blade heights are computed, for hub and tip of stator and rotor, using the correspondent values at these geometric points for ζ_p and g. Since, by definition, this critical blade height corresponds to secondary flow regions with half the blade height, then we can find the level of penetration through:

$$p = 0.5\frac{h_{cr}}{h} \tag{7.52}$$

This value may never be above 50%, since it is not physically possible. If the computation delivers such a case, the program assumes a value of 50%.

Linear Distribution

For the linear distribution case we have figure 7.10.

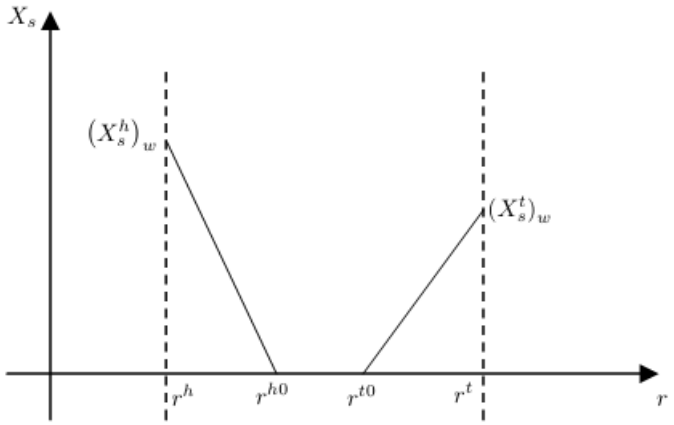

Figure 7.10: *Secondary loss linear distribution*

r^{h0} and r^{t0} are the points where the secondary losses exist no more. They are defined as:

$$r^{h0} = r^h + p^h h \tag{7.53a}$$

$$r^{t0} = r^t - p^t h \tag{7.53b}$$

where p^h and p^t are the levels of penetration for the hub and tip, respectively.

The equation that describes the right hand side curve (next to the tip) is:

$$X_s^t = \left(X_s^t\right)_{sl} r + \left(X_s^t\right)_b \tag{7.54}$$

where $(X_s^t)_{sl}$ is the slope and $(X_s^t)_b$ is the point where the curve touches the X_s axis.

Knowing that the point $\left(r^{t0}, 0\right)$ belongs to the curve, we can determine $(X_s^t)_b$ as equal to $-\left(X_s^t\right)_{sl} r^{t0}$.

We can determine the slope easily through:

$$\left(X_s^t\right)_{sl} = \frac{(X_s^t)_w}{r^t - r^{t0}} = \frac{(X_s)_w}{p^t h} \tag{7.55}$$

where $(X_s^t)_w$ is the value of the losses on the wall.

Hence we have,

$$X_s^t = \left(X_s^t\right)_w \left(\frac{r - r^{t0}}{p^t h}\right) \tag{7.56}$$

Using the same methodology, we can find the equation for the linear curve at the hub:

$$X_s^h = \left(X_s^h\right)_w \left(\frac{r^{h0} - r}{p^h h}\right) \tag{7.57}$$

Through a simple integration we can determine the value of $(X_s^t)_w$.

$$\int_{r^h}^{r^t} (X_s)_{CC}\, dr = \int_{r^{t0}}^{r^t} \left(X_s^t\right)_w \left(\frac{r - r^{t0}}{p^t h}\right) dr + \int_{r^h}^{r^{h0}} \left(X_s^h\right)_w \left(\frac{r^{h0} - r}{p^h h}\right) dr \tag{7.58}$$

In the equation above $(X_s)_{CC}$ is the average of the values found for hub and tip in the secondary losses correlation of [14], $\left(X_s^h\right)_{CC}$ and $(X_s^t)_{CC}$, respectively.

We here define K as

$$K = \frac{\left(X_s^h\right)_{CC}}{(X_s^t)_{CC}} \tag{7.59}$$

We extrapolate this relation to the integrals of the two curves of the hub and tip, so that the possible asymmetric effect of the secondary losses may be felt after its redistribution. This results in:

$$K = \frac{\int_{r^h}^{r^{h0}} \left(X_s^h\right)_w \left(\frac{r^{h0}-r}{p^h h}\right) dr}{\int_{r^{t0}}^{r^t} \left(X_s^t\right)_w \left(\frac{r-r^{t0}}{p^t h}\right) dr} \tag{7.60}$$

Hence, we can take equation 7.58 and rewrite it as:

$$\int_{r^h}^{r^t} \left(X_s\right)_{CC} dr = (1+K) \int_{r^{t0}}^{r^t} \left(X_s^t\right)_w \left(\frac{r-r^{t0}}{p^t h}\right) dr \tag{7.61}$$

This will lead us to $\left(X_s^t\right)_w = \frac{(2X_s)_{CC}}{p^t(1+K)}$.

Hence, we have the final equation describing the right hand-side linear curve on figure 7.10.

$$X_s^t = \frac{2\left(X_s\right)_{CC}}{p^t\left(1+K\right)} \left(\frac{r-r^{t0}}{p^t h}\right) \tag{7.62}$$

The same can be computed for the hub equation, with the following result:

$$X_s^h = \frac{2K\left(X_s\right)_{CC}}{p^h\left(1+K\right)} \left(\frac{r^{h0}-r}{p^h h}\right) \tag{7.63}$$

Parabolic Distribution

For the parabolic distribution case, we have figure 7.11.

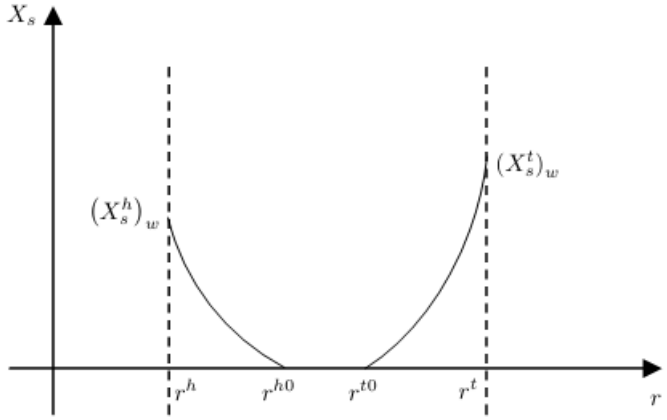

Figure 7.11: *Secondary loss parabolic distribution*

The figure shows two parabolic curves, one for the hub and another for the tip, with the latter expressed by the following equation:

$$X_s^t = A^t r^2 + B^t r + C^t \tag{7.64}$$

Taking the point $\left(r^{t0}, 0\right)$ and substituting we find $C = -A^t {r^{t0}}^2 - B^t r^{t0}$.

The equation is then described as:

$$X_s^t = A^t \left(r^2 - {r^{t0}}^2\right) + B^t \left(r - r^{t0}\right) \tag{7.65}$$

For the sake of simplicity, we assume that this parabolic function has one zero only, and we can write,

$$\frac{dX_s^t}{dr}\left(r^{t0}\right) = 0 \Rightarrow 0 = 2A^t r^{t0} + B^t \Rightarrow B^t = -2A^t r^{t0} \tag{7.66}$$

Also, we know, just like in the linear distribution, that $X_s^t(r^t) = (X_s^t)_w$. Hence, we present the parabolic equation with one unknown only, the value on the wall.

$$X_s^t = \frac{(X_s^t)_w}{{p^t}^2 h^2} \left(r - r^{t0}\right)^2 \tag{7.67}$$

In the same fashion, we can write the equation for the parabolic equation at the hub.

$$X_s^h = \frac{\left(X_s^h\right)_w}{{p^h}^2 h^2} \left(r - r^{h0}\right)^2 \tag{7.68}$$

Integrating as before we have:

$$\int_{r^h}^{r^t} (X_s)_{CC}\, dr = \int_{r^{t0}}^{r^t} \frac{(X_s^t)_w}{{p^t}^2 h^2} \left(r - r^{t0}\right)^2 dr + \int_{r^h}^{r^{h0}} \frac{\left(X_s^h\right)_w}{{p^h}^2 h^2} \left(r - r^{h0}\right)^2 dr \tag{7.69}$$

Just as in equation 7.60, we can write the following equation in order to account for the asymmetry in the secondary losses distribution.

$$K = \frac{\int_{r^h}^{r^{h0}} \frac{\left(X_s^h\right)_w}{{p^h}^2 h^2} \left(r - r^{h0}\right)^2 dr}{\int_{r^{t0}}^{r^t} \frac{(X_s^t)_w}{{p^t}^2 h^2} \left(r - r^{t0}\right)^2 dr} \tag{7.70}$$

Using equations 7.70 and 7.69 we arrive at the expression for $(X_s^t)_w$ and hence for the curve equation.

$$X_s^t = \frac{3\,(X_s)_{CC}}{(1+K)\,p^t} \frac{\left(r - r^{t0}\right)^2}{{p^t}^2 h^2} \tag{7.71}$$

Using the same process for the hub equation we arrive at:

$$X_s^h = \frac{3K\,(X_s)_{CC}}{(1+K)\,p^h} \frac{\left(r - r^{h0}\right)^2}{{p^h}^2 h^2} \tag{7.72}$$

These equations are only valid for their own domain $\left[r^h, r^{h0}\right]$ and $\left[r^{t0}, r^t\right]$, for the hub and tip, respectively, for both linear and parabolic distributions. This procedure is valid for both stator and rotor.

7.2.4 Annulus Losses

In [14] the annulus losses are given by the sum of 3 different annulus losses parameters. Two of these parameters are related to the existence of cavities. For the best design possible, cavities should not be. Hence, these two parameters are null. The other parameter concerns the flow expansion. Since the hub and tip radii do not vary throughout the stator, this parameter would only affect the rotor. However, since the design control enforces $\frac{h_3}{h_2} < 1.2$, we know from the start that this expansion will deliver a very small annulus loss factor, that would have a negligible impact on the total losses. For these reasons, the annulus losses are not taken into account.

7.2.5 Leakage Losses

Leakage losses are the third main source of loss in a turbine (Craig & Cox [14]). These can occur over blade tips, around shrouding, through disc balance holes, etc.. The equation below gives the reduction of blading efficiency due to tip clearance losses when compared to the blading efficiency for zero tip clearance, that is, the efficiency calculated before, comprising profile and secondary losses.

$$\Delta\eta_k = F_k \frac{A_k}{A_t} \eta_{\substack{zero \\ clearance}} \tag{7.73}$$

[14] tells us that this equation must be multiplied by a factor of 1.5 in case of an unshrouded turbine, which we assume to never be the case, in order to have an efficiency as high as possible. The efficiency debit factor F_k is taken from the following plot (figure 7.12).

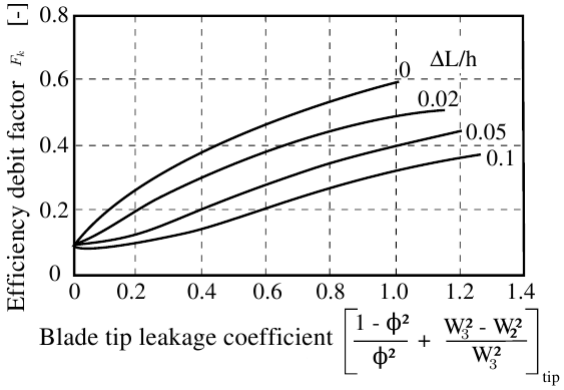

Figure 7.12: *Shrouded efficiency loss [14][15]*

This was calculated using tip values, as required by the plot, using the mean between the velocities at inlet and outlet of the rotor for the computation of ϕ_R. As for W_2 and W_3, they represent the relative velocities at inlet and outlet of the rotor. ΔL, the tip clearance was defined by the rule of thumb that $\Delta L = 0.007h$. However, this may not be feasible due to machining limitations. Thus, a minimum limit of 0.2 mm was imposed. A_k, the total effective area of clearance was calculated as $A_k = t^t \Delta L$, whilst A_t, the total blade throat area, was calculated as $A_t = \frac{t^t + t^h}{2} h$. This last formula corresponds to the area of trapezium, whereas the first corresponds to the area of a rectangle, an approximation therefore, although a good one, since for such a small ΔL the increase in throat size from blade height tip to the clearance tip is negligible. With all these data we are able to calculate $\Delta\eta_k$. We now proceed to its distribution. We assume the clearance losses affect 30% of the blade height, with higher loss at the tip (the value $\Delta\eta_k$), in a linear distribution until we reach zero at a point 30% of the blade height away from the tip. We must first convert X (at this point the sum of profile and secondary loss) to η, using equation 3.45b. Then, we can use the formula on equation 7.73, using $\eta_{\substack{zero \\ clearance}}$ at the tip, to compute $\Delta\eta_k$. The linear distribution was achieved by assigning different weights q_i to each of the points. Therefore, at the tip, q_i must yield 1, whereas at a point 30% of the blade height away from the tip, q_i must yield 0. Hence, we get, for each point i, an efficiency debit,

$$\Delta\eta_{ki} = \Delta\eta_k q_i \tag{7.74}$$

For each point, we get a final efficiency of,

$$\eta_i = \eta_{\substack{zero \\ clearance\, i}} - \Delta\eta_{ki} \tag{7.75}$$

Finally, we can convert the loss back to X, again using equation 3.45b, and we may proceed to the NISRE calculation.

7.3 NISRE

The NISRE (non-isentropic simple radial equilibrium) takes into account the losses in the turbine. These losses are calculated from [14], as presented before. The original radial equilibrium equation is

$$\frac{dh_0}{dr} - T\frac{ds}{dr} = \frac{V_\theta}{r}\frac{d\left(rV_\theta\right)}{dr} + V_x\frac{dV_x}{dr} \tag{7.76}$$

As already referred, the first term is zero. The term $T\frac{ds}{dr}$ is the one that shall be modelled using [14]. Taking the equation above we can write,

$$\frac{V_\theta}{r}\frac{d\left(rV_\theta\right)}{dr} + V_x\frac{dV_x}{dr} + T\frac{ds}{dr} = 0 \tag{7.77}$$

Further manipulation will yield,

$$V_x dV_x = -\frac{V_\theta}{r}\frac{d\left(rV_\theta\right)}{dr} - T\frac{ds}{dr} \tag{7.78}$$

Looking at the equation above, we observe that the term of the left-hand side and the first term of the right-hand side of the equation is the same as for ISRE (equation 7.2). Hence, we can just take the expressions for the integrals already found in ISRE and join the term $-T\frac{ds}{dr}$. Therefore we will have, for each of the tangential velocities distributions,

$$\text{Free Vortex Design: } V_{2_x} = \sqrt{V_{2_x}^{m\,2} - 2\int_{r_2^m}^{r_2} T_2\frac{ds_S}{dr}dr} \tag{7.79a}$$

$$\text{Constant DR Design: } V_{2_x} = \sqrt{-2A^2\left(r_2^2 - r_2^{m\,2}\right) + 4AB\ln\left(\frac{r_2}{r_2^m}\right) - 2\int_{r_2^m}^{r_2} T_2\frac{ds_S}{dr}dr + V_{2_x}^{m\,2}} \tag{7.79b}$$

$$\text{Exponential Design: } V_{2_x} = \sqrt{-2A^2\ln\left(\frac{r_2}{r_2^m}\right) - 2AB\left(\frac{1}{r_2} - \frac{1}{r_2^m}\right) - 2\int_{r_2^m}^{r_2} T_2\frac{ds_S}{dr}dr + V_{2_x}^{m\,2}} \tag{7.79c}$$

$$\text{Free Vortex Design: } V_{3_x} = \sqrt{V_{3_x}^{m\,2} - 2\int_{r_3^m}^{r_3} T_3\frac{ds_R}{dr}dr} \tag{7.80a}$$

$$\text{Constant DR Design: } V_{3_x} = \sqrt{-2A^2\left(r_3^2 - r_3^{m\,2}\right) - 4AB\ln\left(\frac{r_3}{r_3^m}\right) - 2\int_{r_3^m}^{r_3} T_3\frac{ds_R}{dr}dr + V_{3_x}^{m\,2}} \tag{7.80b}$$

$$\text{Exponential Design: } V_{3_x} = \sqrt{-2A^2\ln\left(\frac{r_3}{r_3^m}\right) + 2AB\left(\frac{1}{r_3} - \frac{1}{r_3^m}\right) - 2\int_{r_3^m}^{r_3} T_3\frac{ds_R}{dr}drV_{3_x}^{m\,2}} \tag{7.80c}$$

On the other hand, the tangential velocities expressions are the same (equations 7.33 and 7.34).

For each radial position r, the integral $\int_{r^m}^{r} T\frac{ds}{dr}dr$ must be evaluated carefully. Whereas when we have an $r > r^m$ the integral remains as it is, when $r < r^m$ we must observe that $\int_{r^m}^{r} T\frac{ds}{dr}dr = -\int_{r}^{r^m} T\frac{ds}{dr}dr$. Given the relation between the axial velocity and $T\frac{ds}{dr}$, we must now relate the losses on [14] with $T\frac{ds}{dr}$. The basis for this connection are the expressions below, taken from [10], where we can relate the losses

calculated on [14] with the absolute velocity at the exit of the stator and the relative velocity at the exit of the rotor.

$$X = \frac{V_{2_s}^2 - V_2^2}{V_2^2} \tag{7.81}$$

Which yields,

$$V_2^2 = \frac{V_{2_s}^2}{(1 + X_S)} \tag{7.82}$$

The result is identical for the rotor exit:

$$W_3^2 = \frac{W_{3_s}^2}{(1 + X_R)} \tag{7.83}$$

More important for our case though, is expressing this in terms of loss of total pressure. As in [10], we can write the total pressure loss coefficient as:

$$\text{Stator: } \omega_S = \frac{p_{01} - p_{02}}{\rho_2 \frac{V_2^2}{2}} \tag{7.84a}$$

$$\text{Rotor: } \omega_R = \frac{p_{02}^r - p_{03}^r}{\rho_3 \frac{W_3^2}{2}} \tag{7.84b}$$

According to [10], the total pressure loss coefficient is related to the kinetic loss coefficient ξ, that has the same definition as X (from the Craig & Cox correlation), through:

$$\text{Stator: } \omega_S = X_S \left(1 + \kappa \frac{M_2^2}{2}\right) \tag{7.85a}$$

$$\text{Rotor: } \omega_R = X_R \left(1 + \kappa \frac{(M_3^r)^2}{2}\right) \tag{7.85b}$$

7.3.1 Entropy Increase Stator

The procedure for finding p_0 loss and the associated $\frac{ds}{dr}$ is presented below. These results will be needed for the calculation of the mean axial velocity that satisfies the mass flow in each of the sections.

For each radial position r_2, the increase in entropy can be found at the stator exit using first equation 7.85a to find ω and then equation 7.84a to find a new p_{02} distribution.

We can hence calculate Δs_S. According to [10] we have,

$$\Delta s_S\,(r_2) = -R \ln\left(\frac{p_{02}\,(r_2)}{p_{01}}\right) \tag{7.86}$$

For the calculation of the derivative $\frac{ds_S}{dr}$ we may use equation 3.55a for points in the middle, equation 3.55b for the tip and equation 3.55c for the hub. At this point we are ready to perform the necessary iterations to satisfy the mass flow, as displayed and explained in section 7.3.2.

7.3.2 Calculation Procedure Stator

The NISRE calculation must start with an ISRE calculation, as displayed on 7.1.1. The losses, calculated using [14] and presented in 7.2 follow. The p_0 losses and entropy increase are then calculated for the stator exit, first using ISRE values. At this point we compute $T_2 \frac{ds_S}{dr}$, using on the first iteration ISRE values. After this, we find an absolute axial mean velocity at the stator exit that satisfies the mass flow from the

engine cycle, with a procedure similar to the one on 7.1.1. This procedure must, however, account with the new expressions for the axial velocity. According to [20], the NISRE is an iterative process. We must iterate on the static temperature between the point of calculation of $T_2 \frac{ds_S}{dr}$ and the final results after the mass flow has been satisfied, until convergence. Also, this iterative cycle is inside a bigger iterative cycle starting on the entropy increase. Therefore, these results from the mass flow cycle are also used to be fed back to the entropy increase calculation, until convergence on p_{02}. The equations for the mass flow cycle are reproduced below.

$$T_2(r_2) = T_{01} - \frac{1}{2c_p}\left(V_{2_x}^2(r_2) + V_{2_\theta}^2(r_2)\right) \tag{7.87a}$$

$$p_2(r_2) = p_{02}(r_2)\left(\frac{T_2(r_2)}{T_{01}}\right)^{\frac{\kappa}{\kappa-1}} \tag{7.87b}$$

$$\rho_2(r_2) = \frac{p_2(r_2)}{RT_2(r_2)} \tag{7.87c}$$

$$\dot{m} = \int_{r_2^h}^{r_2^t} 2\pi r_2 \rho_2(r_2) V_{2_x}(r_2) dr \tag{7.87d}$$

After finding the new velocity distribution, we will forcedly have new distributions of the aerothermodynamic quantities. These distributions are fed back to the beginning of the respective cycles, until convergence.

7.3.3 Entropy Increase Rotor

The following calculations that will now be presented are not used directly in the loss at the stator exit, but they will rather be used to calculate p_{02}^r, which is needed to compute the losses at the rotor exit. All values of the stator exit used at this point come from the converged NISRE solution for the stator.

$$W_{2_x}(r_2) = \sqrt{V_2^2(r_2) - V_{2_\theta}^2(r_2)} \tag{7.88}$$

$$W_{2_\theta}(r_2) = V_{2_\theta}(r_2) - \Omega r_2 \tag{7.89}$$

$$M_2^r(r_2) = \sqrt{\frac{W_{2_x}^2(r_2) + W_{2_\theta}^2(r_2)}{\kappa R T_2(r_2)}} \tag{7.90}$$

$$p_{02}^r(r_2) = \frac{p_2(r_2)}{\left(1 + \frac{\kappa-1}{2} M_2^{r\,2}(r_2)\right)^{\frac{-\kappa}{\kappa-1}}} \tag{7.91}$$

We also need to compute the new T_{03}^r, needed for the mass flow cycle of the rotor.

$$T_{03}^r = T_2(r_2) + \frac{W_2^2(r_2)}{2c_p} - \frac{U_2^2(r_2)}{2c_p} + \frac{U_3^2(r_3)}{2c_p} \tag{7.92}$$

We are now in position to compute $\frac{ds}{dr}$ for the rotor. Just like in the stator case, we use equation 7.85b to calculate ω and then 7.84b in order to compute p_{03}^r.

$$\Delta s_R\left(r_3\right) = c_p \ln\left(\frac{T_{03}^r\left(r_3\right)}{T_{02}^r\left(r_2\right)}\right) - R\ln\left(\frac{p_{03}^r\left(r_3\right)}{p_{02}^r\left(r_2\right)}\right) \tag{7.93}$$

We note that the expression for Δs_R depends also on the total relative temperature ratio, unlike in the stator case, since we have $T_{01} = T_{02}$ but $I_2 = I_3$, which results in $T_{02}^r \neq T_{03}^r$.

Once again, for the calculation of the derivative $\frac{ds_R}{dr}$ we may use equation 3.55a for points in the middle, equation 3.55b for the tip and equation 3.55c for the hub.

7.3.4 Calculation Procedure Rotor

The NISRE calculation for the rotor follows the same steps as for the stator. However, relative quantities are used for the calculation of the static temperature, since T_{03}^r, calculated in equation 7.92, must be taken as a reference for the NISRE calculation for the rotor. Once again, this computation must start with an ISRE calculation, as displayed on 7.1.1. The losses, calculated using [14] and presented in 7.2 follow. The p_0 losses and entropy increase are then calculated for the rotor exit, using ISRE values in the first computation. We may then compute $T_3\frac{ds_R}{dr}$, once again using ISRE values in the first iteration. A procedure to find an absolute mean axial velocity at the rotor exit that satisfies the mass flow from the engine cycle, similar to the one on 7.1.1, follows. This procedure must, however, account with the new expressions for the axial velocity. Since T_{03}^r will be used to find the static temperature, this means that at every step, an equation will be needed to find W_{3_θ}, just as in the ISRE. Obviously, no equation is needed to find W_{3_x} since this is equal to V_{3_x}. The new static temperature distribution found at the beginning of the cycle is fed back to the point of the $T_3\frac{ds_R}{dr}$ calculation, until convergence. This cycle is inside a bigger cycle, that starts at the entropy increase calculation. Data with the new distributions are fed to the beginning of this cycle, until convergence on p_{03}^r. The equations for the mass flow cycle are reproduced below.

$$W_{3_\theta}(r_3) = V_{3_\theta}(r_3) + \Omega r_3 \tag{7.94a}$$

$$T_3(r_3) = T_{03}^r(r_3) - \frac{1}{2c_p}\left(W_{3_x}^2(r_3) + W_{3_\theta}^2(r_3)\right) \tag{7.94b}$$

$$p_3(r_3) = p_{03}^r(r_3)\left(\frac{T_3(r_3)}{T_{03}^r(r_3)}\right)^{\frac{\kappa}{\kappa-1}} \tag{7.94c}$$

$$\rho_3(r_3) = \frac{p_3(r_3)}{RT_3(r_3)} \tag{7.94d}$$

$$\dot{m} = \int_{r_3^h}^{r_3^t} 2\pi r_3 \rho_3(r_3) V_{3_x}(r_3) dr \tag{7.94e}$$

The results of the NISRE (new distributions for velocity, temperature, pressure, etc.) are computed the same way as the ones of the ISRE, with the difference in the expressions for the absolute axial and tangential velocities and the difference in the use of relative quantities for the rotor.

7.4 Procedure Summary

A summary of the procedure for the radial equilibrium calculation is presented below, in an enumerated list.

1. ISRE calculation;
   (a) $V_{2_x}^m$ calculation;
   (b) $V_{3_x}^m$ calculation;
2. Losses calculation;
   (a) Losses calculation for the stator exit;
   (b) Losses calculation for the rotor exit;
3. NISRE calculation;
   (a) Stator NISRE cycle;
      i. Cycle on entropy increase calculation for the stator exit;
      ii. Cycle on $T_2 \frac{ds_S}{dr}$ calculation;
      iii. New $V_{2_x}^m$ calculation;
   (b) Rotor NISRE cycle;
      i. Cycle on entropy increase calculation for the rotor exit;
      ii. Cycle on $T_3 \frac{ds_R}{dr}$ calculation;
      iii. New $V_{3_x}^m$ calculation;

Chapter 8

Airfoil Selection

After the completion of the NISRE calculation, we proceed to the calculation of the NACA profiles for the turbine. For this purpose, we use the work of James Dunavant and John Erwin [23]. This paper is the only available source for programming a methodical process of airfoil choosing. [23] offers two possible profiles. Only the primary airfoil (named A_3K_7), with a maximum thickness over chord at 20% of the chord, was considered for this methodology, against the secondary airfoil (named $B_1E_1I_1$), which presents the maximum thickness over chord at 20% of the chord. We have the following coordinates for this airfoil in the table on the side (table 8.1). The method of construction of the airfoils using these data is presented in figure 8.1, adapted from [23].

The camber coordinates are given in percentage of the chord. These values of y_c are for a $C_{l_0} = 1.0$ (C_{l_0} is the *camber, expressed as design lift coefficient of isolated airfoil*[23]). Calculating x_c for each blade control point i is direct. We must simply compute:

$$(x_c)_i = x_c \frac{c}{100} \tag{8.1}$$

The chords are the same for the entire vane and blade. Hence, x_c is the same at all control points of stator and rotor.

x_c	y_c	x_t	y_t
0	0	0	0
0.5	0.397	1.25	3.469
1.25	0.836	2.5	4.972
2.5	1.428	5.0	6.918
5.0	2.359	10	9.007
10	3.689	15	9.827
15	4.597	20	10.000
20	5.217	25	9.899
25	5.623	30	9.613
30	5.852	35	9.106
35	5.936	40	8.594
40	5.897	45	7.913
45	5.753	50	7.152
50	5.516	55	6.339
55	5.200	60	5.500
60	5.814	65	4.661
65	4.367	70	3.848
70	3.870	75	3.087
75	3.328	80	2.406
80	2.746	85	1.830
85	2.133	90	1.387
90	1.485	95	1.101
95	0.801	100	0
100	0		

Table 8.1: *Airfoil coordinates*

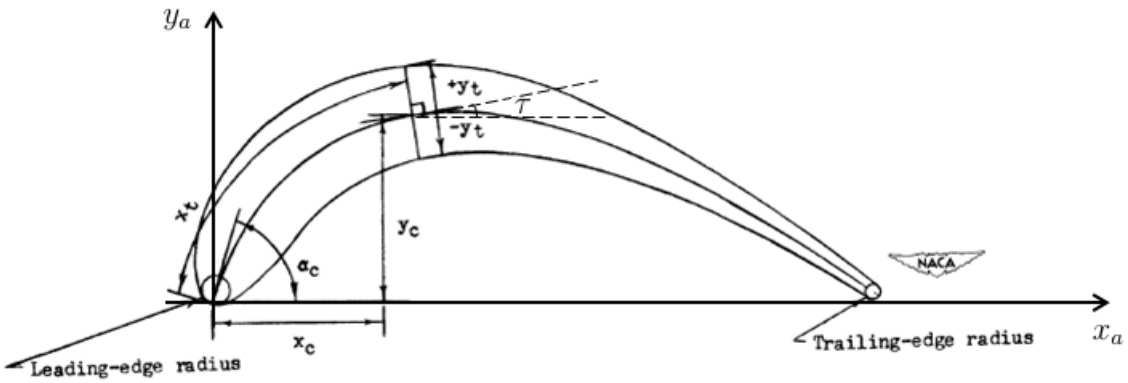

Figure 8.1: *Method of blade construction*

At this point of the camber coordinates calculation, we are only missing y_c. This quantity, besides depending on the chord, also depends on C_{l_0}. In fact, we can write:

$$(y_c)_i = (C_{l_0})_i (y_c)_{C_{l_0}=1.0} \frac{c}{100} \tag{8.2}$$

C_{l_0} can be computed knowing the control section turning angle. From [23], we have,

$$(\Delta\alpha)_c = \Delta\alpha + (\Delta\alpha)_{induced} + (\Delta\alpha)_{deviation} = \arctan\left(C_{l_0}\left(\frac{dy_c}{dx_c}\right)_{0.5}\right) - \arctan\left(C_{l_0}\left(\frac{dy_c}{dx_c}\right)_{95}\right) \tag{8.3}$$

The A_3K_7 airfoil has the following quantities defined:

$$\left(\frac{dy_c}{dx_c}\right)_{0.5} = 0.5657 \tag{8.4a}$$

$$\left(\frac{dy_c}{dx_c}\right)_{95} = -0.2017 \tag{8.4b}$$

We also have the turning angle information from the NISRE. Therefore, we must find $(\Delta\alpha)_{induced}$ and $(\Delta\alpha)_{deviation}$ in order to compute $(\Delta\alpha)_c$ and then iterate on C_{l_0} until convergence. In order to accomplish this, we use figures 8.2 and 8.3.

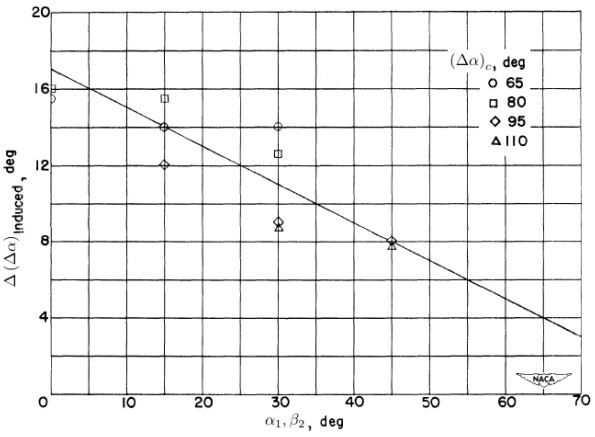

Figure 8.2: *Induced turning angle* [°]

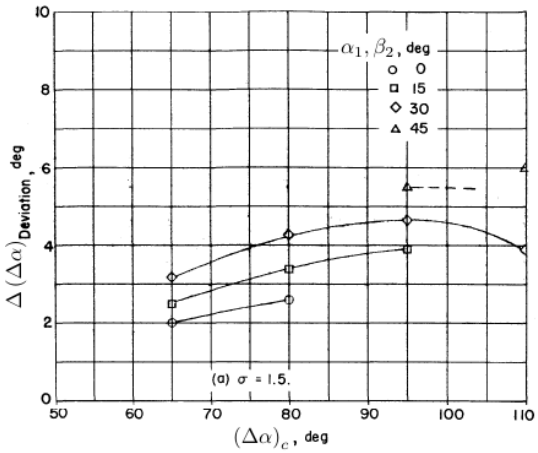

Figure 8.3: *Deviation turning angle* [°]

They both depend on the flow inlet angle and on the turning. Both plots were created based on a solidity of 1.5. [23] also offers the same kind of plots for a solidity of 1.8. These solidities correspond

to pitch over chord ratios of 0.67 and 0.56, respectively. If we look into figure 5.3, the plot that gives optimum pitch to chord ratios at zero trailing edge thickness, we observe that a value of 0.67 on this plot is much more representative of the general trend of pitch to chord ratios, whilst a value of 0.56 sits on the extreme minimum of the plot. Therefore, the plots for a solidity of 1.5 were chosen for this airfoil selection. Hence, simply by using the velocity triangles we can compute $(\Delta\alpha)_{induced}$ and $(\Delta\alpha)_{deviation}$. We now can calculate $(\Delta\alpha)_c$ through equation 8.3. Using the right-hand side of this equation we can find C_{l_0} for each control point. This is done through an iterative cycle by varying C_{l_0} until reaching convergence, in a similar method to that described by table 7.1. Finally, we can apply equation 8.2 in order to find $(y_c)_i$ and complete the coordinates that define the camber line.

The coordinates for the thickness are given in percentage of the mean line length. The mean line length of an airfoil can be calculated using the coordinates x_c and y_c, with j representing the points that make up the airfoil at the control point i.

$$(ml)_i = \sum_j \sqrt{\left((x_c)_i^{j+1} - (x_c)_i^j\right)^2 + \left((y_c)_i^{j+1} - (y_c)_i^j\right)^2} \tag{8.5}$$

Therefore, we can already calculate $(x_t)_i$:

$$(x_t)_i = x_t \frac{(ml)_i}{100} \tag{8.6}$$

y_t is tabulated for a thickness over chord of 20%. Hence, in order to achieve other thickness over chord ratios, we must simply multiply by the ratio of the desired thickness to 20%. Therefore, the calculation of y_t for each blade control point i can be summed up in the following fashion:

$$(y_t)_i = y_t \frac{(ml)_i}{100} \frac{t/c}{0.2} \tag{8.7}$$

Two more quantities can be calculated for the airfoils according to [23]. The trailing edge radius, TER, which depends only on the chord. Therefore, we will have one value for the stator and another for the rotor.

$$TER = 0.01c \tag{8.8}$$

The leading edge radius, LER, depends not only on the chord, but also on the mean line length. Hence, we will have different values for each control point at stator and rotor. According to [23], the leading edge radius is given by equation 8.9.

$$(LER)_i = 0.04407(ml)_i \left(\frac{\frac{t}{c}\frac{c}{(ml)_i}}{20} \right)^2 \tag{8.9}$$

8.1 Coordinates in the airfoil reference frame

We have now successfully calculated the airfoil x_c, y_c, x_t and y_t coordinates. Using figure 8.1 we can calculate the coordinates of the upper and lower surfaces of the airfoil. Given that the information for the camber and the one for the thickness are in two different reference frames, we must first find a correspondence between the camber coordinates and the thickness coordinates of the airfoil.

Using $\sqrt{\left((x_c)_i^{j+1} - (x_c)_i^j\right)^2 + \left((y_c)_i^{j+1} - (y_c)_i^j\right)^2}$, we are able to create a new set of points over the camber line, the same points that were used to compute the mean line length. These points, unlike $(x_t)_i$ that were calculated as a percentage of the camber line length, are calculated as a function of the camber line coordinates and hence associated with the position of x_c. We now have a connection between the thickness coordinates and the camber line coordinates. Using the values of $(y_t)_i$ and their correspondence to $(x_t)_i$, we can find new values of the thickness distribution for the newly calculated points over the camber line using a simple linear distribution for each new point. We now have coordinates for the camber line with a thickness distribution associated to those points. Given that the thickness is distributed along the camber line on perpendiculars, we must calculate the derivative of the camber line at each point, in order to find the angle τ, shown in figure 8.1, necessary to calculate the final coordinates. The derivatives were achieved with second order finite differences, given by equations 3.56. From the derivatives, we can calculate τ using,

$$\tau = \arctan\left(\frac{dy}{dx}\right) \tag{8.10}$$

The geometric transformation of the coordinates is given below, as a direct result of figure 8.1.

$$\begin{bmatrix} x_a^u \\ y_a^u \\ x_a^l \\ y_a^l \end{bmatrix} = \begin{bmatrix} 1 & 0 & -\sin(\tau) \\ 0 & 1 & \cos(\tau) \\ 1 & 0 & \sin(\tau) \\ 0 & 1 & -\cos(\tau) \end{bmatrix} \begin{bmatrix} x_c \\ y_c \\ y_t^n \end{bmatrix} \tag{8.11}$$

8.2 Coordinates in the vane/blade reference frames

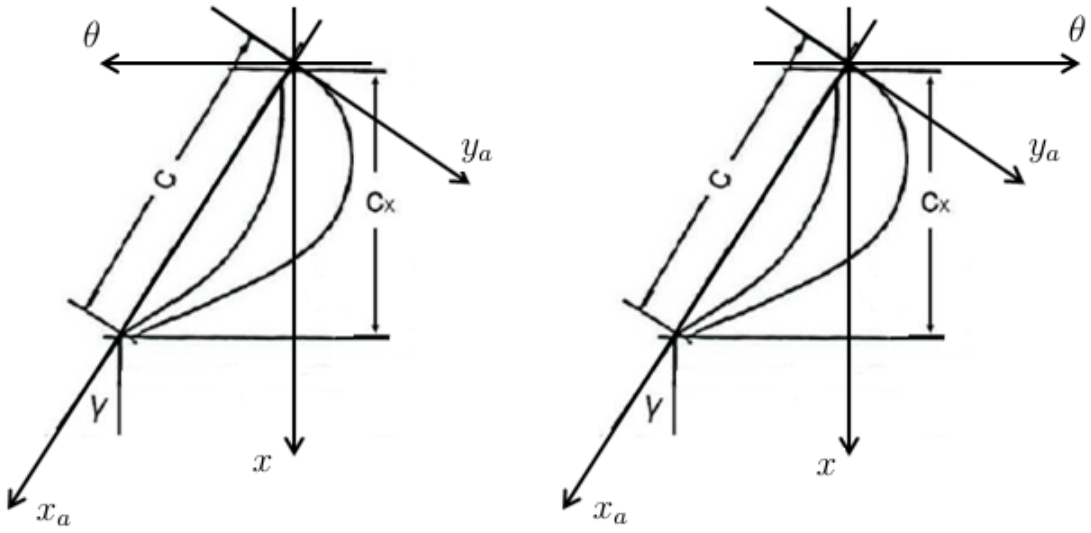

Figure 8.4: *Reference frame transformation for the stator (left) and for the rotor (right)*

The vane/blade coordinates must account with the stagger angle previously calculated. The leading edge is the reference point in this transformation, that is, the only point kept unchanged and common to all

airfoils. According to figure 8.4, we can relate the coordinates in the airfoil reference frame to the turbine reference frame using the following transformation matrices. It is important to notice that due to the different convention as to which tangential direction is positive between stator exit and rotor exit, two figures are needed, one for the stator (left) and another for the rotor (right).

$$\text{Stator:} \quad \begin{bmatrix} x \\ \theta \end{bmatrix} = \begin{bmatrix} \cos(\gamma) & \sin(\gamma) \\ \sin(\gamma) & -\cos(\gamma) \end{bmatrix} \begin{bmatrix} x_a \\ y_a \end{bmatrix} \tag{8.12a}$$

$$\text{Rotor:} \quad \begin{bmatrix} x \\ \theta \end{bmatrix} = \begin{bmatrix} \cos(\gamma) & \sin(\gamma) \\ -\sin(\gamma) & \cos(\gamma) \end{bmatrix} \begin{bmatrix} x_a \\ y_a \end{bmatrix} \tag{8.12b}$$

These equations are applied to both the upper and lower surfaces of the airfoil.

Chapter 9

Worked Out Example

In this chapter, an example of a run of the program is presented in a summed up way. The inputs of this program will be fully presented, otherwise an understanding of the results would not be possible. However, for the sake of simplicity given the large amount of data delivered, only a representative selection of the results is presented.

9.1 Inputs

The inputs of this run are presented in table 9.1. As already discussed, many of the values presented in the table are no more than guesses that will be changed by the computation. The numbering presented in the pressure and temperature inputs concerns the engine numbering, since this type of initial data given concerns the engine. As input, a free vortex tangential velocity distribution was chosen, along with a constant mean line radius geometry and a linear distribution of the secondary losses.

Symbol	*Value*	*Symbol*	*Value*
p_{01}	1.01325e5 Pa	Π_{cc}	0.99
T_{01}	288 K	M_3	0.8
Π_c	13	R_p $minimum$	0.32
T_{03}	1600 K	R_p $maximum$	0.4
p_{05}	1.01325e5 Pa	η_S	0.92
k_{air}	1.4 $J/(kg.K)$	α_2 $minimum$	70°
cp_{air}	1000 $J/(kg.K)$	α_2 $maximum$	74°
k_{gas}	1.3 $J/(kg.K)$	U	470 m/s
cp_{gas}	1240 $J/(kg.K)$	η_R	0.87
P_{pt}	1.1e6 W	β_3 $minimum$	60°
η_c	0.85	β_3 $maximum$	65°
η_{cc}	0.99	$\frac{r_h}{r_t}$	0.9
η_{gg}	0.87	$\frac{h}{c}_S$	0.65
η_{pt}	0.87	$\frac{h}{c}_R$	1.15
η_m	0.99	t/c	0.1
LHV	43e6 J/kg		

Table 9.1: *Example Inputs*

9.2 Results

9.2.1 1D Design

The following results are obtained in the 1D design phase:

p_{01}	T_{01}	p_{02}	T_{02}	p_{03}	T_{03}
1304052.75 Pa	1600.00 K	1214520.13 Pa	1600.00 K	464425.53 Pa	1309.86 K

Table 9.2: *Absolute total temperatures and pressures for the turbine*

$\dot{m}$	R_h	R_p	ϕ	ψ	P_{gg}	P_{av}	η_{TT}
2.63 kg/s	0.41192	0.32400	0.40862	1.61148	945341.06 W	949827.84 W	0.855412

Table 9.3: *Design characterization quantities*

$\beta_2 + \beta_3$	M_2	M_2^r	M_3	M_3^r	U^m
109.66°	0.9547	0.3751	0.4158	0.9194	472.50 m/s

Table 9.4: *Controlled quantities*

Section	α	β	V_x	V_θ	V	W	h
1	0°	0°	118.83 m/s	0 m/s	118.83 m/s	0 m/s	0.011478 m
2	73.77°	44.66°	193.07 m/s	663.30 m/s	690.83 m/s	271.44 m/s	0.011478 m
3	20.80°	65.00°	267.77 m/s	101.73 m/s	286.45 m/s	633.60 m/s	0.012589 m

Table 9.5: *Velocity triangles and section height*

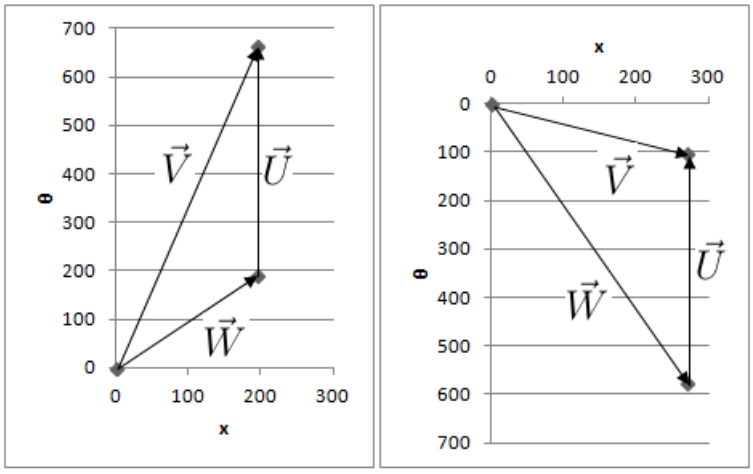

Figure 9.1: *Velocity triangles for the 1D design (stator and rotor exits, respectively)*

Component	c_x	c	t_e	g	N_b
Stator	0.009202 m	0.017659 m	0.000500 m	0.015225 m	45.000000
Rotor	0.009162 m	0.010464 m	0.000419 m	0.007447 m	92.000000

Table 9.6: *Turbine Geometry*

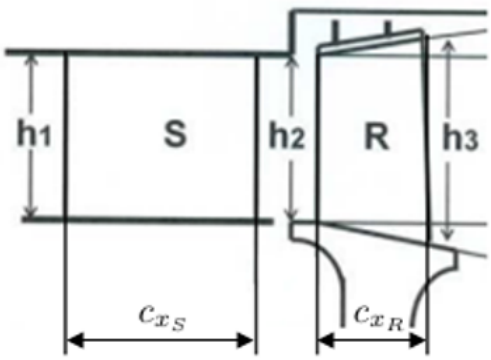

Figure 9.2: *Turbine stage geometry*

As we can see, the program was able to deliver a feasible 1D design, respecting all the design control guidelines.

9.2.2 2D Design

Even though the results are printed at 21 evenly spaced lines, the results shown here display only the hub, mid-span and tip, for the sake of simplicity. The console gave no warnings during the process, meaning that a Free Vortex design is feasible for the previously presented input.

Location	α_2	α_3	β_2	β_3	V_{2_x}	V_{2_θ}	V_2	
Hub	75.64858°	25.85632°	54.64838°	68.06439°	179.14 m/s	700.15 m/s	722.70 m/s	
Mid	74.88686°	24.54417°	46.80614°	68.79562°	179.14 m/s	663.30 m/s	687.06 m/s	
Tip	74.13057°	23.35161°	36.54424°	69.50318°	179.14 m/s	630.14 m/s	655.10 m/s	
Location	V_{3_x}	V_{3_θ}	V_3	W_{2_θ}	W_2	W_{3_θ}	W_3	R_h
Hub	222.78 m/s	107.97 m/s	247.57 m/s	252.52 m/s	309.61 m/s	553.19 m/s	596.37 m/s	0.34013
Mid	222.78 m/s	101.73 m/s	244.91 m/s	190.80 m/s	261.71 m/s	574.23 m/s	615.94 m/s	0.40436
Tip	222.78 m/s	96.18 m/s	242.66 m/s	132.77 m/s	222.97 m/s	595.96 m/s	636.24 m/s	0.45939

Table 9.7: *ISRE velocity triangles*

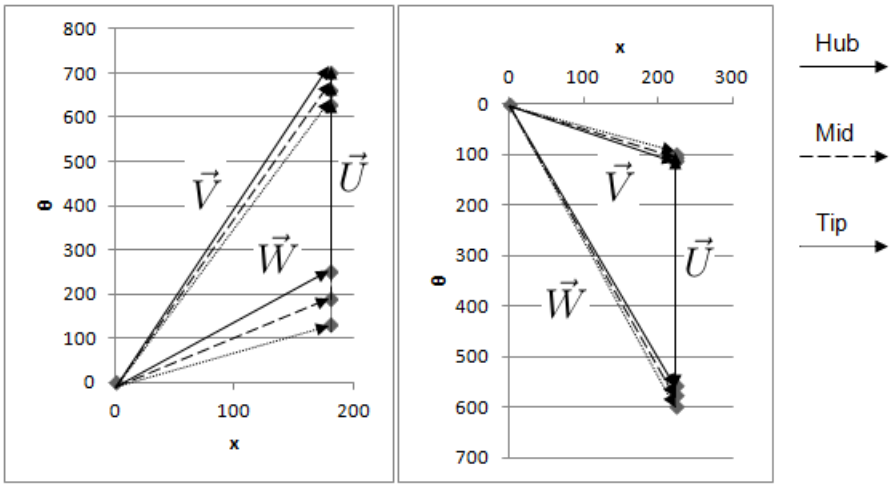

Figure 9.3: *Velocity triangles for the ISRE (stator and rotor exits, respectively)*

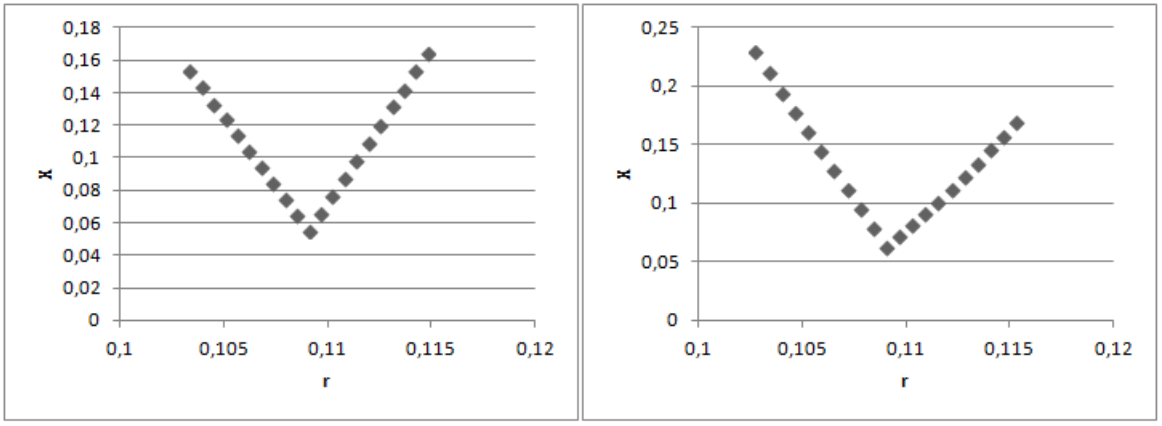

Figure 9.4: *Total losses according to the Craig & Cox correlation (stator and rotor exits, respectively)*

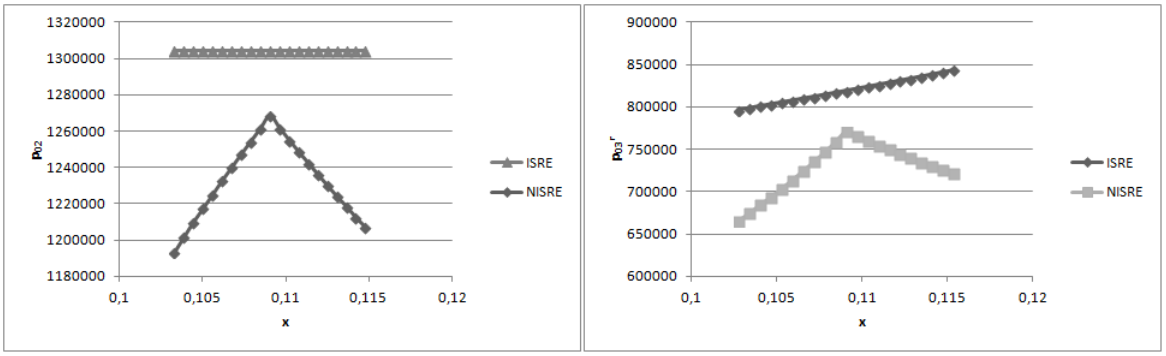

Figure 9.5: *Pressure loss in p_{02} and p_{03}^r, respectively*

Location	α_2	α_3	β_2	β_3	V_{2_x}	V_{2_θ}	V_2	
Hub	81.15660°	36.32783°	66.66553°	75.13516°	108.93 m/s	700.15 m/s	708.57 m/s	
Mid	69.75809°	17.52055°	37.95632°	60.69901°	244.60 m/s	663.30 m/s	706.96 m/s	
Tip	76.93869°	27.05939°	42.24549°	72.46659°	146.19 m/s	630.14 m/s	646.87 m/s	
Location	V_{3_x}	V_{3_θ}	V_3	W_{2_θ}	W_2	W_{3_θ}	W_3	R_h
Hub	146.83 m/s	107.97 m/s	182.25 m/s	252.52 m/s	275.01 m/s	553.19 m/s	572.35 m/s	0.34242
Mid	322.26 m/s	101.73 m/s	337.94 m/s	190.80 m/s	310.21 m/s	574.23 m/s	658.48 m/s	0.40990
Tip	188.29 m/s	96.18 m/s	211.43 m/s	132.77 m/s	197.48 m/s	595.96 m/s	624.99 m/s	0.46344

Table 9.8: *NISRE velocity triangles*

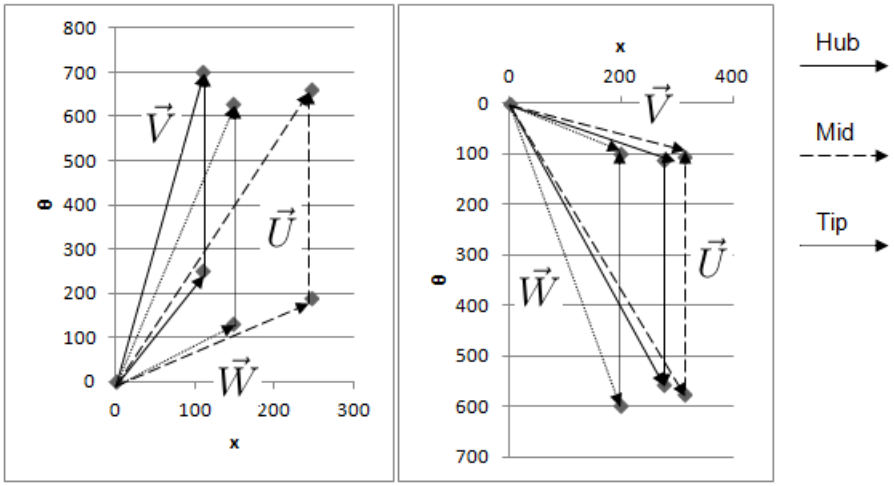

Figure 9.6: *Velocity triangles for the NISRE (stator and rotor exits, respectively)*

The radial distribution of the velocity triangles is quite visible, especially in the NISRE, with the losses delivering a strong effect over the velocity triangles.

9.2.3 3D Geometry

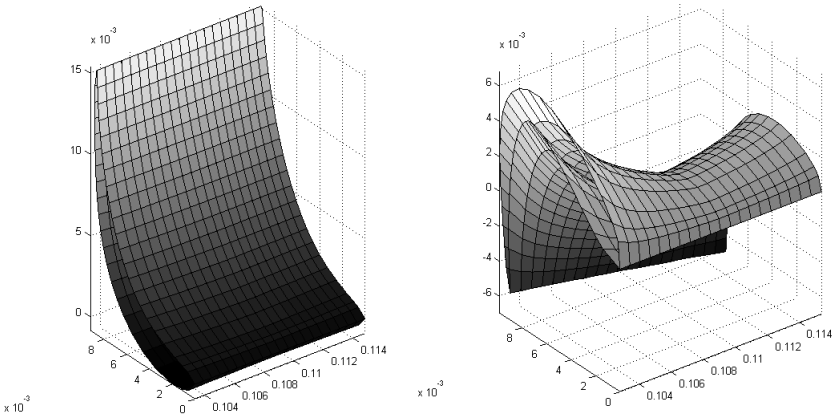

Figure 9.7: *Airfoils (stator and rotor, respectively)*

These airfoils were plotted using the software MATLAB, by running the code printed automatically by the C program for this purpose.

Chapter 10

Conclusions

A solid knowledge of the design process needed for the preliminary design of a turbine exists. On the other hand, a compilation of this process under an automated program that contains the knowledge necessary for such a design was needed. Hence, the major contribution of this thesis is the program hereby developed, that can obtain a feasible and realistic preliminary design of a turbine through a fast computation process, up to a 3D geometry, including a process of choosing airfoils for different radial control sections.

The process is based on a methodical design procedure, that can take the data regarding the engine this turbine is part of, and deliver a full 3D geometry. There are several sections to this design procedure. In the beginning, we have the ECA and then the MLA, which includes loss calculation and therefore the computation of a realistic value for the total to total efficiency, essential for assuring a truthful design. The MLA calculation process was based on the data delivered from the ECA, always taking into account the aerothermodynamic expressions that were presented in Chapter 3. Therefore, the MLA includes the calculation of all aerothermodynamic quantities at mean radius. This enables us to jump to RET, a full 2D design, first isentropic, with the ISRE, and then with loss calculation and subsequent non-isentropic radial equilibrium, NISRE. The RET calculation main focus is finding the axial velocity at mean radius that satisfies the mass flow value found at the ECA. Meanwhile, after the ISRE, the loss values for the turbine were computed, including profile, secondary and leakage losses. For this purpose, the Craig & Cox correlation [14] was implemented, since it represents a complete and methodical process to compute the loss. Finally, the airfoils along the radius were computed using [23], again because this represents a methodical, and hence programmable way of computing airfoil coordinates, thus calculating a 3D geometry.

The results of this program were compared against another program in development at VKI that delivers similar outputs, though with a different calculation process. The results were very comparable, and therefore satisfying, enabling us to trust the results delivered by this program.

The results delivered were also satisfying in the control of design aspect. Upon analysis of the results of the 1D design, the action of the design control is visible, enabling the program to deliver more realistic and feasible results. The 2D design, with three tangential velocity distributions, proved capable of analysing which velocity distributions are feasible or not, and also of restarting the 2D calculation for a

new tangential velocity distribution when needed.

Therefore, the objective of this thesis, meeting the need for an automatic, fast and reliable way to perform a preliminary design of a one-stage axial gas turbine in order to produce a 3D geometry ready for optimization, is considered accomplished.

10.1 Recommendations and possible improvements

Even though the objective of this thesis is considered accomplished, several possible improvements could be implemented into this program. One possible improvement is taking control points at streamlines during the 2D analysis, instead of evenly spaced points (this includes considering the existence of radial velocity). The calculation will deliver more accurate and smoother results in what concerns the radial distribution of aerothermodynamic quantities. The use of more points for the calculation would also be an improvement, helping to minimize computation errors, always associated to the use of certain tools employed in this thesis, such as numerical integration and differentiation, processes which can themselves be updated to more complex formulas that may deliver a smaller numerical error. Another possible improvement is the inclusion of more tangential velocity distributions, hence giving the user more options to choose from. For this purpose, also new loss calculation methods can be implemented.

In the end, the desired use of this program would be the coupling with a turbine optimizer, therefore creating a tool capable of delivering a full and complete turbine design.

Bibliography

[1] *"aeolipile", Encyclopædia Britannica, Encyclopædia Britannica Online, Encyclopædia Britannica Inc., 2014. Web. 06 Jul. 2014, http://www.britannica.com/EBchecked/topic/7176/aeolipile*

[2] *"Sir Charles Algernon Parsons". Encyclopædia Britannica, Encyclopædia Britannica Online, Encyclopædia Britannica Inc., 2014. Web. 06 Jul. 2014, http://www.britannica.com/EBchecked/topic/444719/Sir-Charles-Algernon-Parsons*

[3] *"Massachusetts Institute of Technology Gas Turbine Lab". Web.mit.edu., Web. 06 Jul. 2014, http://web.mit.edu/aeroastro/labs/gtl/early_GT_history.html*

[4] *TESLA, N., Our Future Motive Power, Web. 06 Jul. 2014, http://www.tfcbooks.com/tesla/1931-12-00.htm*

[5] *BOWIE, D., Cruising Turbines of the 'Y100' naval propulsion machinery, Web. 06 Jul. 2014, http://www.hazegray.org/navhist/canada/systems/propulsion/y100/y100.pdf*

[6] *"BusinessWeek", Frank Whittle: A Daredevil Who Built Jets, 02 May 2004, Web. 06 Jul. 2014, http://www.businessweek.com/stories/2004-05-02/frank-whittle-a-daredevil-who-built-jets*

[7] *GOLLEY, J., et. al., Genesis of the jet: Frank Whittle and the invention of the jet engine, Volume 12, Airlife, 1996*

[8] *QIN, X., et. al., Optimization for a steam turbine stage efficiency using a genetic algorithm, Elsevier, 2003*

[9] *HORLOCK, J.H., Axial Flow Turbines, Fluid Mechanics and Thermodynamics, Butterworths, 1966*

[10] *SIEVERDING, C.H., Advanced Course on Turbines, Von Karman Institute for Fluid Dynamics, 2014*

[11] *COHEN, H., ROGERS, G.F.C., SARAVANAMUTTOO, H.I.H., Gas Turbine Theory, 4^{th} Edition, T.J. Press, 1996*

[12] *MORAN, M.J., SHAPIRO, H.N., Fundamentals of Engineering Thermodynamics: SI Edition, 6^{th} Edition, John Wiley & Sons, 2009*

[13] *ARTS, T., Private communication, 2014*

[14] *CRAIG, H.R.M., COX, H.J.A., Performance Estimation of Axial Flow Turbines, Proceedings of the Institute of Mechanical Engineers, Vol 185, 32, 1970-71*

[15] *MÜLLER, L., Design Exercise: Cold Rig, Von Karman Institute for Fluid Dynamics, April 2011*

[16] *McDONALD, P.W., Aerodynamic Design of a Gas Turbine, Course Note 93, von Karman Institute for Fluid Dynamics, 1975*

[17] *TRAUPEL, W., Termische Turbomachinen, Bd. 1: Thermodynamisch-strömungstechnische Berechnung, Springer Verlag Berlin, 1977*

[18] *HOLLIGER, K., Weiterentwicklung von Dampfturbinen-Schaufelungen, Escher Wyss Mitt. 33. Jg., 75-81, 1960*

[19] *WEI, N., Significance of Loss Models in Aerothermodynamic Simulation for Axial Turbines, Royal Institute of Technology, 2000*

[20] *CHAUVIN, J., Meridional Flow in Axial Turbomachines, Course Note 99, von Karman Institute for Fluid Dynamics, 1977*

[21] *DEJC, M.E., TROJANOVSKIJ, B.M, Untersuchung und Berechnung axialer Turbinenstufen, VEB Verlag Berlin1, 1973*

[22] *KACKER, S.C., OKAPUU, U., A mean line prediction method for axial turbine efficiency, J. Engineering for Power, Vol. 104, 1982*

[23] *DUNAVANT, J., ERWIN, J., Investigation of a Related Series of Turbine-Blade Profiles in Cascade, National Advisory Committee for Aeronautics, December 7, 1953*

[24] *DE BOOR, C., CONTE, S.D., Elementary Numerical Analysis - An algorithm Approach,* 3^{rd} *Edition, McGraw-Hill, 1980*

[25] *HIRSCH, C., Numerical Computation of Internal and External Flows - Volume 1 Fundamentals of Computational Fluid Dynamics,* 2^{nd} *Edition, Butterworth-Heinemann, 2007*

[26] *DAMAS, L., Linguagem C, FCA - Editora de Informática, 1999*